Missouri S&T Library and Learning Resources

Scholars' Mine

Masters Theses

Student Theses and Dissertations

Fall 2017

Well log interpretation and 3D reservoir property modeling of Maui-B field, Taranaki Basin, New Zealand

Aziz Mennan

Follow this and additional works at: https://scholarsmine.mst.edu/masters_theses

 Part of the Petroleum Engineering Commons

Department:

Recommended Citation

Mennan, Aziz, "Well log interpretation and 3D reservoir property modeling of Maui-B field, Taranaki Basin, New Zealand" (2017). *Masters Theses*. 7722.
https://scholarsmine.mst.edu/masters_theses/7722

This thesis is brought to you by Scholars' Mine, a service of the Missouri S&T Library and Learning Resources. This work is protected by U. S. Copyright Law. Unauthorized use including reproduction for redistribution requires the permission of the copyright holder. For more information, please contact scholarsmine@mst.edu.

WELL LOG INTERPRETATION AND 3D RESERVOIR PROPERTY MODELING OF THE MAUI-B FIELD, TARANAKI BASIN, NEW ZEALAND

by

AZIZ MENNAN

A THESIS

Presented to the Faculty of the Graduate School of the

MISSOURI UNIVERSITY OF SCIENCE AND TECHNOLOGY

In Partial Fulfillment of the Requirements for the Degree

MASTER OF SCIENCE IN PETROLEUM ENGINEERING

2017

Approved by

Dr. Ralph E. Flori, Advisor
Dr. Kelly Liu
Dr. Mingzhen Wei

Copyright 2017

AZIZ MENNAN

All Rights Reserved

ABSTRACT

Maui-B is one of the largest hydrocarbon–producing fields in the Taranaki Basin. Many previous works have estimated reservoir volume. This study uses 3D property modeling, which is one of the most powerful tools to characterize lithology and reservoir fluids distribution through the field. This modeling will help in understanding the reservoir properties and enhancing the production by selecting the best location for future drilling candidates. In this study, 3D seismic, core, and well log data were used to build and define a structural model, facies analysis, and petrophysical parameters. After well log interpretation and petrophysical parameter calculations, each parameter was upscaled. Then, geostatistical methods, including Gaussian simulation, variogram, and Monte Carlo simulation, were used to build a 3D property model. A thousand 3D models were constructed and performed for each parameter; the outputs were implemented into Monte Carlo simulation, which is a highly reliable method regarding accuracy to calculate the mean of each parameter. Then, the volume of the reservoir was estimated. In this study, integration of seismic interpretation and well logs defined the depth and thickness of the hydrocarbon reservoir through the field. Gamma ray, spontaneous potential, and caliper logs were used for depth correlation and identifying permeable zones. As a result, five different lithofacies, where sandstone and claystone distribution have the significant impact on reservoir quality were identified. The matrix identification (MID) method was used for porosity correction, which showed effective porosity ranges of 15–25%. Moreover, permeability was estimated as 79–3700 mD, where all results were calibrated using available core data. Furthermore, 9% to 40% water saturation was estimated using the resistivity logs and core data. Finally, oil and gas in place were estimated.

ACKNOWLEDGMENTS

I would like to express my gratitude to my advisor, Dr. Ralph E. Flori, for his guidance and support. I would also like to thank my committee members, Dr. Kelly Liu and Dr. Minghzen Wei, for their help and suggestions in completing my study.

Sincere thanks to my father Fahri Mennan, my mother Ayse Mennan, and my sisters Azize Mennan, Elif Mennan. I would also like to thank to my uncle Isa Bal for his support to me all of my life; I am very lucky to have an uncle like him. I would also like to thank Aslihan Vuruskan, who supported to me during all of my graduate studies, and last I would like to thank my elementary school teacher Belgin Altug for teaching me to read and write and her support during all of my life.

I am very grateful to Turkish Petroleum Corporation for funding my Master of Science study. I would also like to acknowledge New Zealand Petroleum and Minerals for providing data for my thesis study, and Mr. Aamer Alhakeem for sharing his study experiences and his support.

I am honored to mention our first president Mustafa Kemal Ataturk, who supported younger generations for science and education every despite with limited facilities. I thank him everlasting.

DEDICATION

Dedicated to my father, Fahri Mennan who helped me during my whole life with very limited opportunities and stood by me always unconditionally. My dear father, you were and will be always in my heart.

TABLE OF CONTENTS

Page

LIST OF ILLUSTRATIONS

LIST OF TABLES

1. INTRODUCTION

1.1. OVERVIEW OF THE TARANAKI BASIN

The Taranaki Basin is located in the west part of the North Island of New Zealand. It is a huge hydrocarbon producing basin that is mostly offshore and with an area of 100,000 km^2. The Taranaki Basin is the only hydrocarbon–producing sedimentary basin in the New Zealand (1). The geologic history of the Taranaki Basin is related to the evolution of the Australia–Pacific plate boundary, which includes encompassing rifting, passive subsidence, compressional tectonics, and late back arc-rift phases. The history of the basin starts from the Late Cretaceous and goes to the Neogene (2). This basin has a very complex morphology because of different kind of tectonic events including crucial normal, reverse, and overthrust faulting (1). The main geological structure for this basin is the Taranaki Fault, which is one of the longest structures of New Zealand's continental crust and Alpine Fault (1). The basin is understood very well from previous hydrocarbon exploration with important geological structure in both offshore and onshore areas (3). This basin's important exploration activities started in the 1950s onshore, and exploration activities still continue, so there is an enormous amount of data available for this area (4). Most of the field discovered in onshore, however the vast portion of the producing fields in offshore. The recoverable reserves of the Tranaki basin are 332 million barrels of oil and 5.2 trillion cubic feet of gas. until the first period of 1996, almost half of the reserves were produced. A significant amount of hydrocarbon from the Taranaki Basin was produced from marine shales and coals from the Late Cretaceous and Paleogene. Currently, the Taranaki Basin has nineteen oil fields, including Maui, Mangahewa, Kapuni, Cardiff/Radno, Turangi/Ohanga, Pohokura, McKee, Tuhua,

Tui, Kupe, Rimu, Maari, Kaimiro, Cheal, Moturoa, Karewa, Ngatoro, Waihapa, and Toko fields (5).

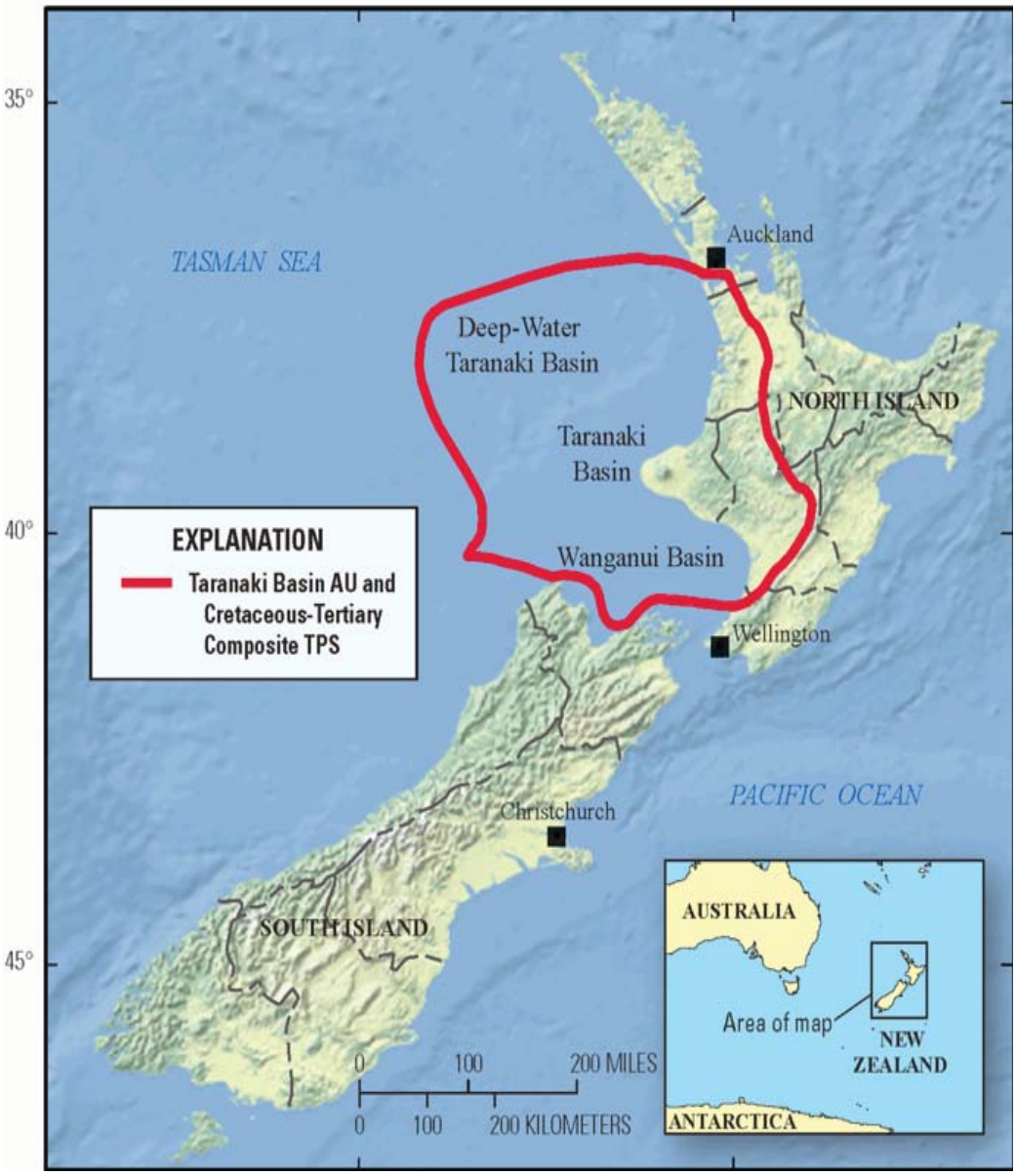

Figure 1.1: Location of Taranaki Basin

1.2. LOCATION OF THE STUDY AREA

The Maui oil and gas field is located 35 km from the south Taranaki coastline. Maui-A and Maui-B are the two primary structural closures for the area. Presently,

the field has the largest hydrocarbon reservoir in New Zealand, which includes $157km^2$ area and 3000 m depth. The west part of the area is bounded by Whikiti Fault and the east part of the area is bounded by the Cape Egmont Fault and the area is divided by two subfields, named the Maui-A and Maui-B fields. The area has been drilled since 1969 by different petroleum companies (6).

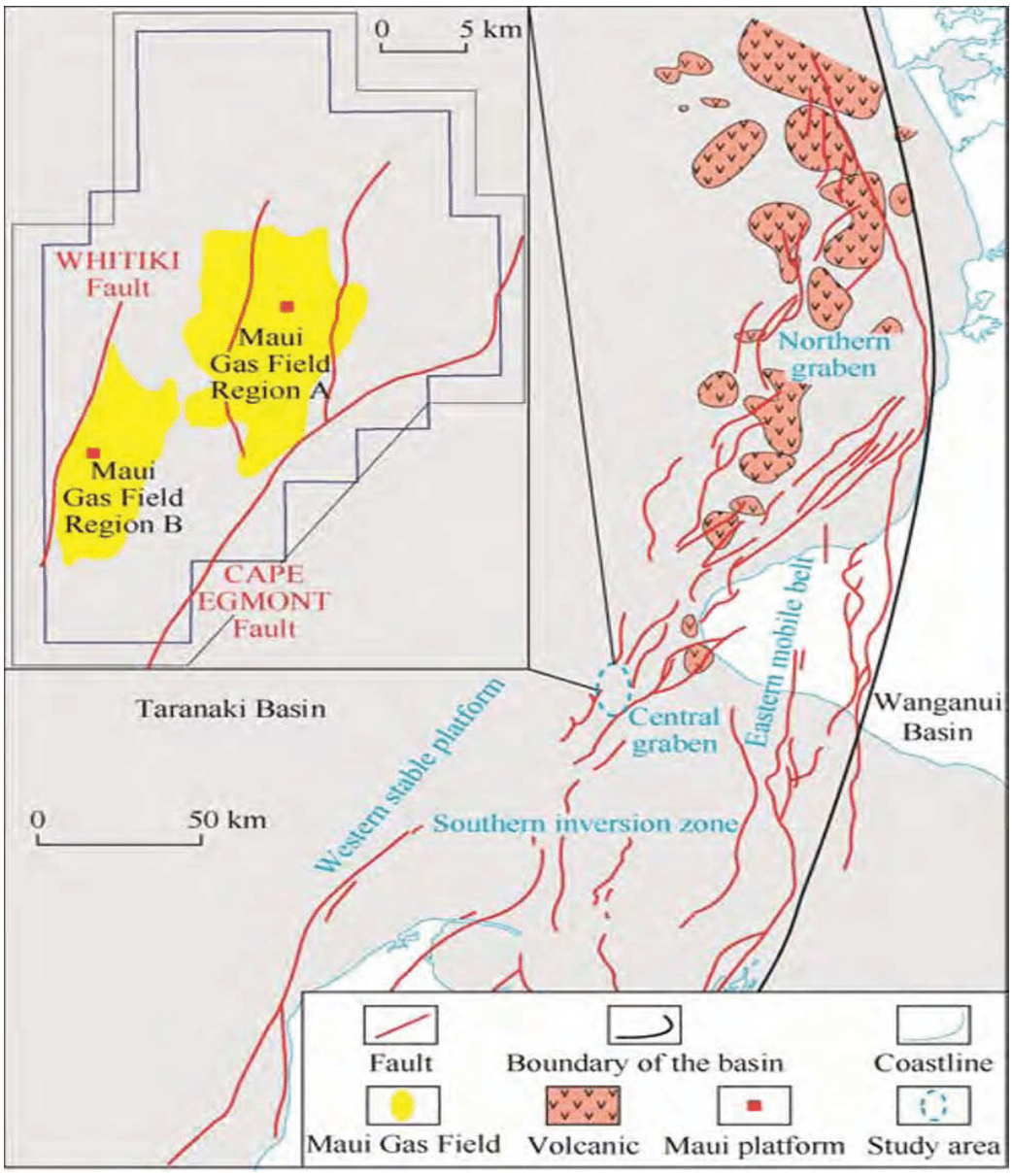

Figure 1.2: Location of Maui Gas Field

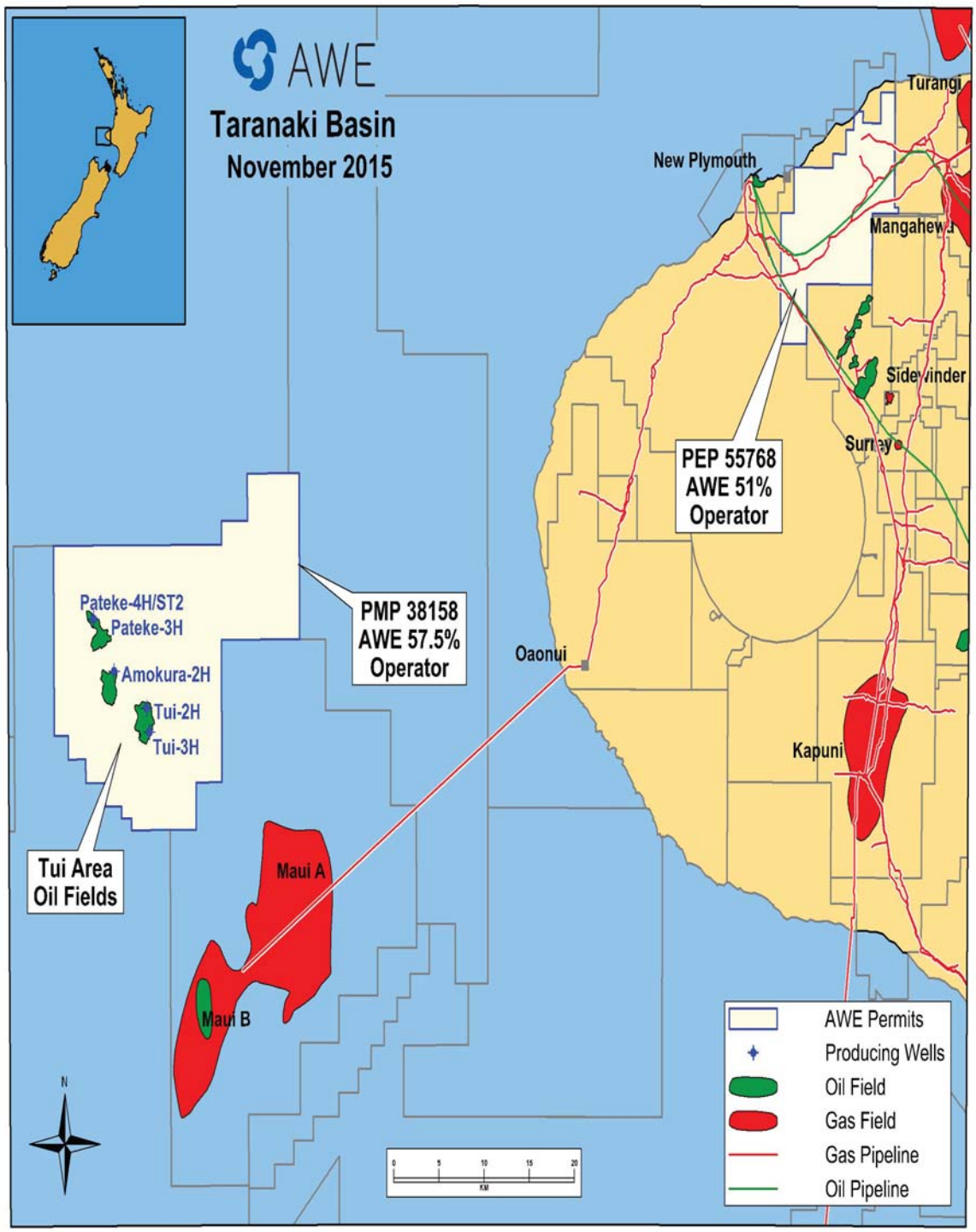

Figure 1.3: Location of Maui A and B Fields

1.3. HISTORY OF THE MAUI FIELD

The Maui field was discovered by the Shell-BP-Todd consortium with the Maui-1 well for Maui-B structure in 1969. The following drilling activity for this area was the Maui-2 and Maui-3 wells for Maui-A structure in 1979. Until 2003, 34 wells were drilled in the Maui field at that time, including 14 development wells in the Maui-A structure, 12 development wells in the Maui-B structure, with eight exploration and appraisal wells. The last exploration activity was in 2006 with two wells in both sides of the Ihi fault in north part of the Maui-A structure. The estimated ultimate recovery is 5.3 tcf gas and 300 million barrel of oil. In producing D Sand zone,
Initial reservoir pressure= 4257 $psig$,
Initial reservoir temperature= 219.5 F,
Bubble point pressure= 4062 $psig$,
Gas gravity= 0.71,
Gas formation volume factor= 0.0049 CF/SCF,
Oil gravity= 0.819,
Oil API= 41.2,
Oil formation volume factor= 1.736 $RBBL/STB$,
Solution gas oil ratio at BP=1548 SCF/STB (6).

1.4. AIM OF THE STUDY

The main purposes of this study is to build a 3D reservoir property model to improve reservoir management, reserve estimation, to understand the field that has complex geometry, to aid decision making, to improve production, to decide drilling scenarios, and guide reservoir simulation research to determine alternative well locations and different production scenarios. In this study, 3D seismic data were used to understand geological settings of the field, define large–scale geological

Table 1.1: Petrophysical Parameters in Maui–7 Well

Depth(m)	ϕ (%)	ρ_b (g/cm^3)	S_w (%)
2713 - 2728	26	2.25	20
2727 - 2738	19.5	2.35	35
2754 - 2766	18	2.37	38
2766 - 2791	26	2.25	6
2793 - 2795	13	2.45	70
2803 - 2804	19.5	2.35	21
2808 - 2810	26	2.25	97
2940 - 2945	28	2.22	0
3010 - 3030	22	2.30	23
3030 - 3035	18	2.37	42
3037 -3040	18	2.37	50
3040 - 3044	20.5	2.33	56
3044 - 3046	20.5	2.33	100

structures, and define cap rock, seal rock, and source rock with structural model. In addition, well log and core data were used to find hydrocarbon zones. Lastly, 3D property models including facies, porosity, permeability, water saturation, and net–to–gross ratio were constructed for detailed visualization in the field area.

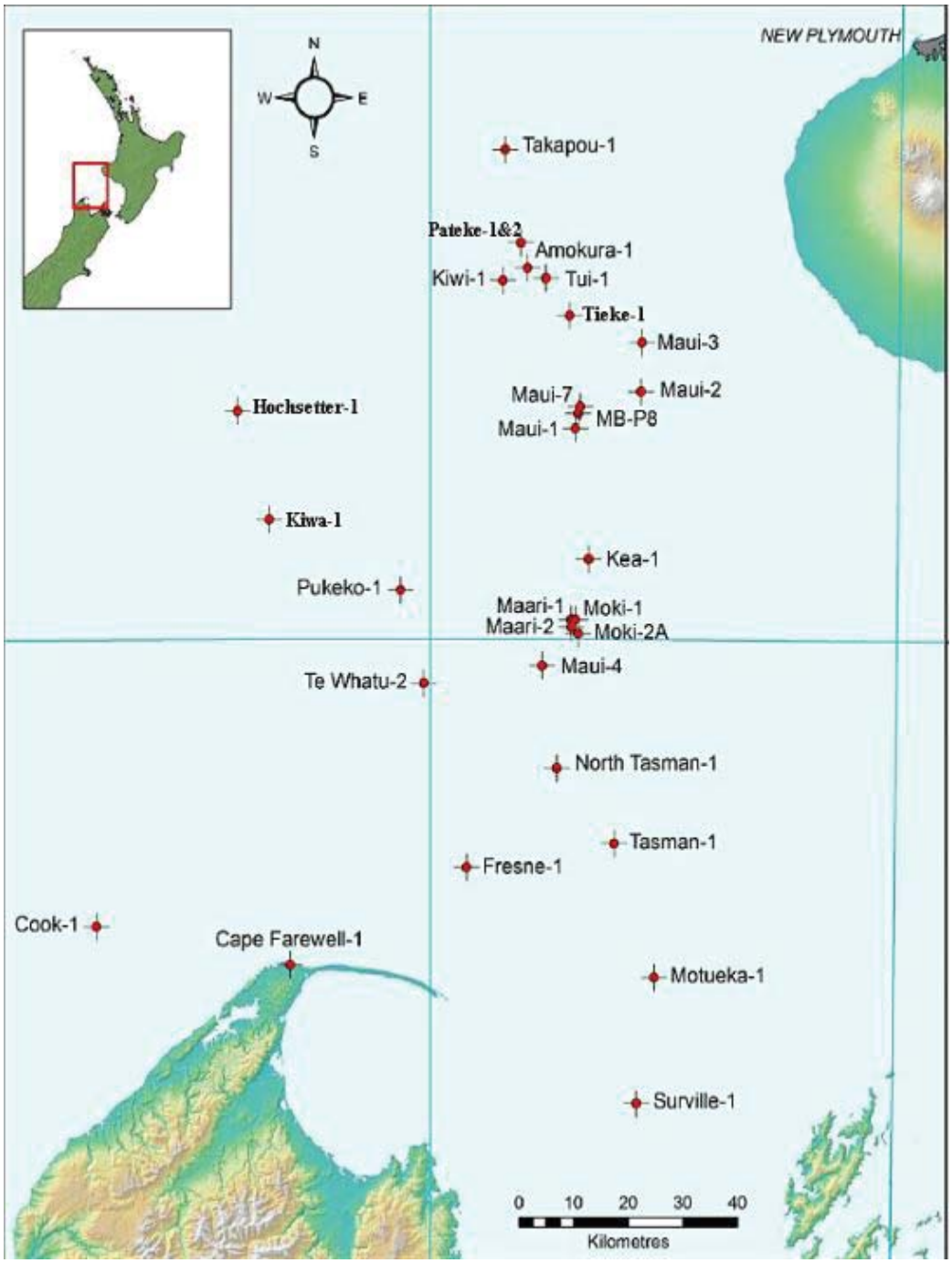

Figure 1.4: Well Locations

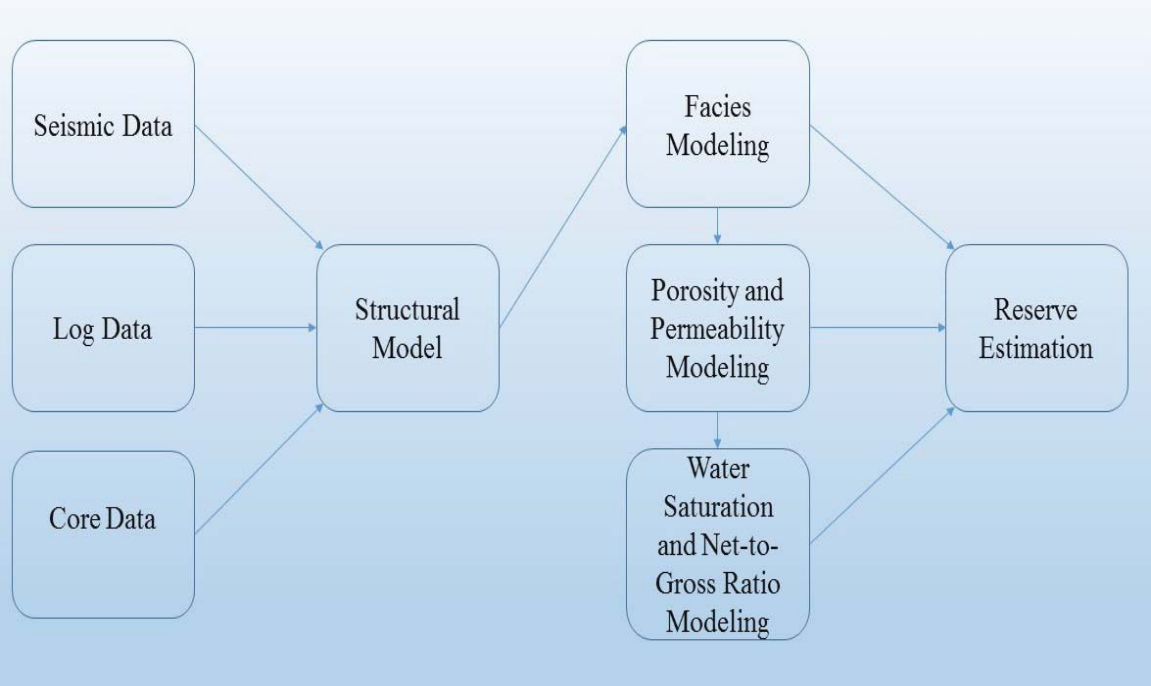

Figure 1.5: Workflow of the Study

2. REGIONAL GEOLOGY

2.1. GEOLOGICAL SETTING AND TECTONIC HISTORY

The Taranaki basin covers around 100 000 km^2 much of which is offshore, located west of the New Zealand's North Island. The basin is overhead the subduction zone betwen Australian Plate and Pacific Plate (Figure 2.1). The most important strictural components of the Taranaki basin are the Western Platform and the Eastern Mobile Belt. After the middle of the Cretaceous, the basin's tectonic history is fairly complicated. Because of this there are many sub–basins, depocentres, and uplift areas in the basin. The Taranaki fault is one of the primary geological structures, which is a Miocene age reverse fault.

Late Cretaceous sediments were deposited within an continental rift system. After rifting, through the Paleocene and Eocene the Taranaki basin evolved. A subbasin evolved on the southeastern side of the basin in the age of Late Eocene. This is related with evolution of the Australia–Pacific plate boundary. The west part of the Taranaki fault intersected with a change in shape of the convergent plate boundary in early Miocene. From beginning to end of the Neogene, the Taranaki basin was part of the Australin plate which is evaolving both active margin, Eastern Mobile Belt, and passive margin, Western Stable Platfrom.

The Taranaki basin's main source rocks are hydrogen rich coals and carbonaceous mudstones in Late Cretaceous to Eocene age. Also most of the oils show some evidence of marine contribution. Well–known reserves deposited in Paleogene shoreline and coastal plain sandstones however producible hydrocarbons in Late Cratecous strata have not been produced so these hydrocarbon zones are potential reservoirs (7).

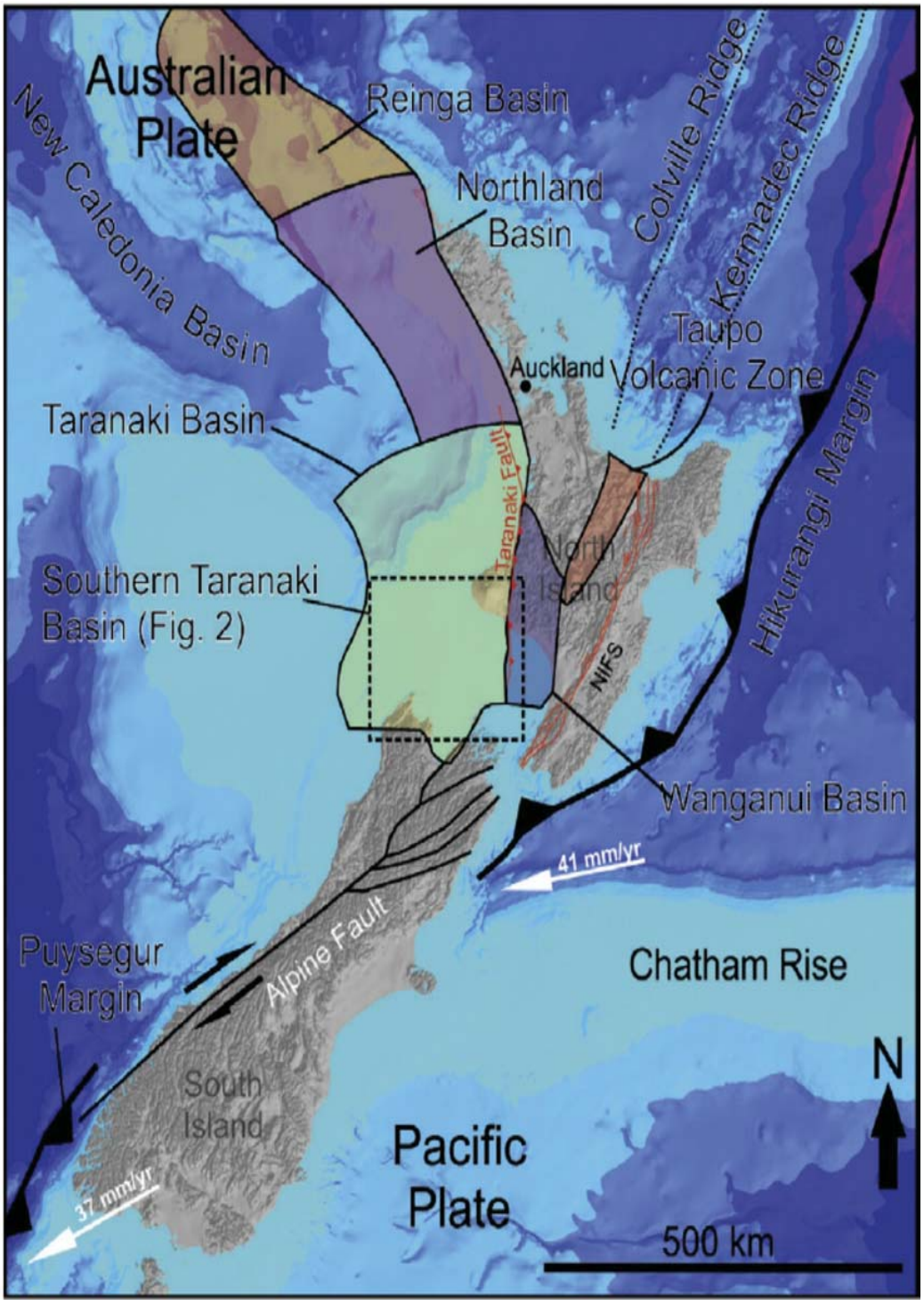

Figure 2.1: Taranaki Basin Location between Australian Plate and Pacific Plate (8)

2.2. GEOLOGICAL STRATIGRAPHY

In this study Kapuni C Sand and Kapuni D Sand formations were considered as a reservoir bearing formations. Kapuni formations are sandstone dominated formations which contains marginal marine and terrestrial facies in Early Eocene age (9).

Kapuni sandstones have different kinds of sandstones from early to middle of the Eocene. The first type of sandstone is medium to coarse grain size, well sorted, and includes quartz–dominated sandstones. The other type of sandstone is fine to medium grain size and has argillaceous sandstones.

The Kapuni formations include a range of lower alluvial plain, delta or coastal plain, and marginal marine lithofacies (10).

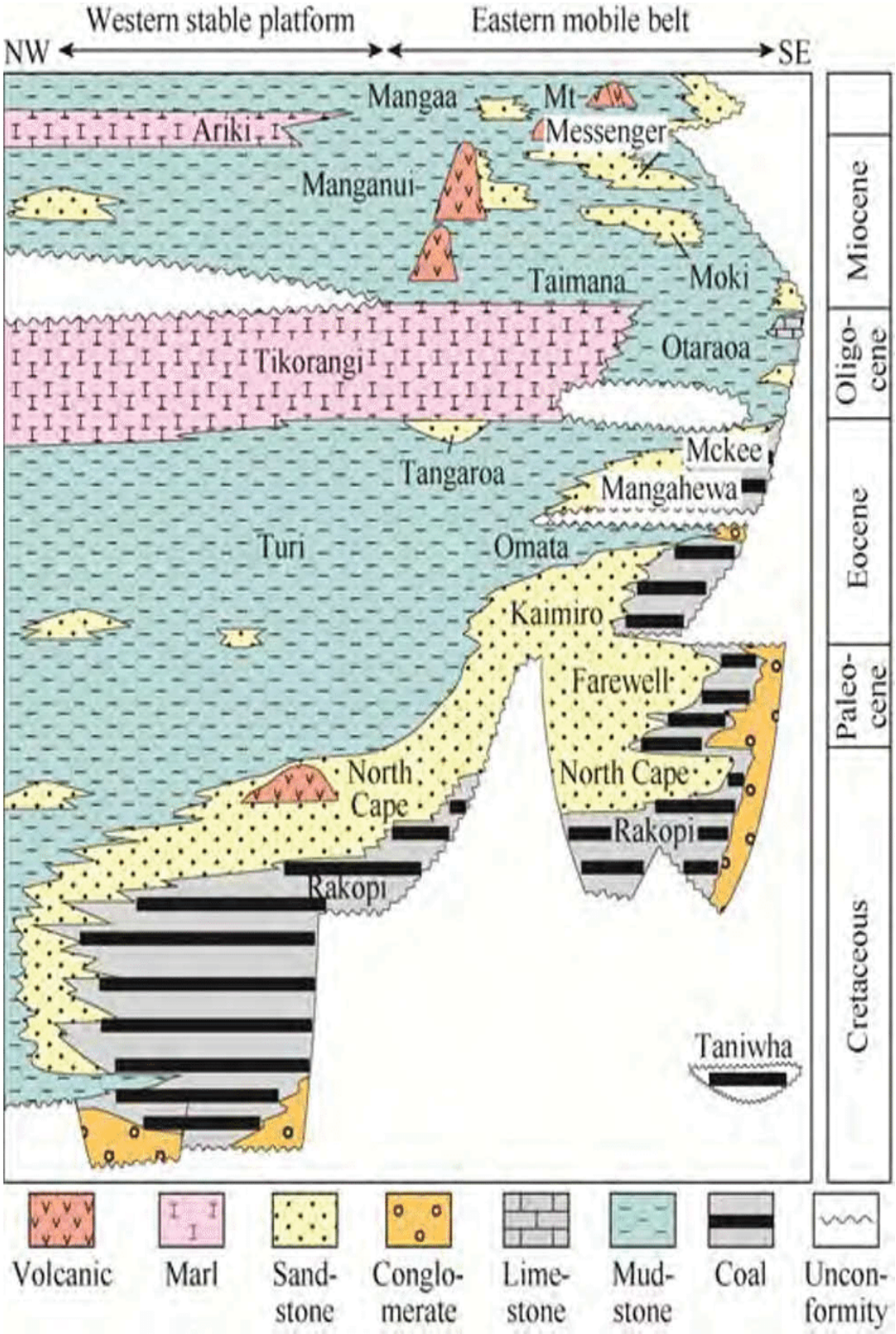

Figure 2.2: Kapuni Formations (11)

3. DATA AND SOFTWARE

Three dimensional seismic data, well log data, and core data were used in this study. Well log data and core data were calibrated for accurate results.

3.1. SEISMIC DATA

Three dimensional seismic data were interpreted to define 3D structural model, faults, and other large scale geological structures.

3.2. WELL DATA

Five different wells are available in Maui-B field and each well has main logs like gamma ray, spontaneous potential, caliper, density, neutron, sonic, and resistivity logs. Using these logs, petrophysical parameters were calculated if core data is not available.

3.3. CORE DATA

Core data were used in this study. Porosity, permeability, and grain density were available in core data. Core data were available for all of the wells; however, it was not available from surface to reservoir zones depth.

3.4. SOFTWARE

Three different software were used in this study.

3.4.1. Kingdom Suite 2015. Kingdom Suite 2015 version was used for seismic interpretation and petrophysical parameter calculations from well logs. After doing these interpretations and calculations, the data were exported from this software and imported to Petrel 2016 software.

3.4.2. Petrel 2016. Petrel 2016 software was improved by Schlumberger company and was used in this study for 3D property modeling, well log analysis, and geostatistical analysis using histograms and crossplots. The software provides different kinds of methods for 3D modeling such as Gaussian simulation and Monte Carlo simulation.

3.4.3. Techlog 2015. Techlog 2015 software was improved by Schlumberger company for petrophysical analysis. In this study, this software were used to do crossplots to obtain porosity, type of lithofacies, and matric density in the formation.

4. WELL LOG INTERPRETATION

Well log interpretation is a powerful tool to understand lithology, petrophysical analysis, fluid saturation, and reserve estimation. Well log interpretation gives more accurate results when the log data is combined with core data. In this study, core data were used to identify five different type of facies where sandstone and claystone distribution have the significant impact on reservoir quality. Gamma ray logs (GR), spontaneous potential logs (SP), and caliper logs were used for the correlation of depth and identification of permeable zones in addition to identifying the same facies in the wells, which have a lack of core data. Porosity logs (density logs, neutron logs, sonic logs) were used to calculate porosity at each point. Then, the matrix identification (MID) method was used to correct porosity to get more accurate results. Moreover, density logs and neutron logs were used to identify gas zones because density logs are overestimated in gas zones, while neutron logs are underestimated in gas zones, to identify gas zones density logs and neutron logs crossover were used. The next step is to identify permeable zones using porosity and water saturation. Resistivity logs were used to obtain water saturation. After obtaining water saturation, both oil and gas saturation can be calculated. To get more reliable results, these calculations were corrected with core data.

4.1. GAMMA RAY (GR) LOG

The gamma ray log, which detects natural radioactive emissions of the rocks to identify lithology, is a passive tool. All of the rocks emit some radiation but shales primarily, so this tool helps to identify shale and non-shale zones. The most important sources of natural radioactivity are the radioactive isotopes of potassium (K40), uranium, and thorium. Radioactivity also depends on the age and deposition

type. Age of the rock plays an important role on the amount of radioactivity; as the rock ages less radiation is emitted. Mostly, clay minerals have more radioactive elements (12). While shale contains higher gamma ray values, sand and carbonates carry low intensity gamma rays. Therefore, intensity of gamma rays is helpful to discriminate shale and non-shale.

4.2. SPONTANEOUS POTENTIAL (SP) LOG

The spontaneous potential (SP) log is a passive log that gives values which are affected by the thickness of the formation, water formation salinity, mud resistivity, mud salinity, and borehole diameter. Mud salinity is often different than formation water salinity, and this salinity difference causes Cl and Na cations to move from high concentration to the low concentration.

A membrane causes diffusion potential buildup and associated current that occurs at the boundaries between the sandstone and the shale. The SP tool will measure this potential at various depth. Therefore, its a useful tool to identify the lithologic boundaries between sandstone and shale, formation correlation, gross lithology estimation, identification of depositional environments, and qualitative indication of porosity and permeability. This tool has some limitations, for example it needs a conductive mud to be run in, good hole conditions, and the sandstone should be permeable, so the SP log is not the best tool to estimate shale. However, it is perfect when it is combined with the GR log. The effect of these factors makes the static spontaneous potential (SSP) value more accurate than the SP value (13). To define deflections the shale baseline must be defined first. After that, deflections can be measured using this shale baseline. If mud filtrate resistivity is higher than water

resistivity, it represents negative deflection. In positive deflection situation, mud filtrate resistivity is lower than water resistivity. Deflections from the shale baseline represents permeable zones (14).

4.3. CALIPER LOG

A caliper log is a mechanical tool that evaluates the borehole environment for logging measurements, determines packer depth, determines cement volume, identifies mud cake buildup, and indicate permeability. Caliper logs can be classified by the number of arms (15). In todays operations, the most common caliper log type is the four arm caliper log. The caliper log is fairly important because the size and shape of the borehole have economic impacts.

The shape and size of the borehole impact most of the areas in petroleum engineering including drilling, completion strategies, effect of the geomechanical forces, image interpretation for geological goals as well as log accuracy (16).

4.4. POROSITY LOGS

There are three types of porosity logs: density logs, neutron logs, and sonic logs. Each of them is used to determine porosity. In addition, combining these logs together ensures more accurate results.

4.4.1. Density Log. The density log is an neutron active tool that measures electron density of the formation, which aims to measure bulk density, identify evaporite minerals, determine gas bearing zones combining with neutron log, and define formation mechanical properties combining with sonic log. Bulk density can read from density log and also porosity can be derived from density log if matrix density and fluid density are known. The oil zone does not significantly affect the density

log, but the gas effect which is overestimated in density log is important because it aids in detecting gas zone boundaries (17).

4.4.2. Neutron Log. The neutron Log is another neutron active tool that measures the formations hydrogen ion concentration. The aim of neutron log interpretation is to detect porosity, lithology identification using sonic log or density log, gas zone indication using density log, and clay content using density. Neutron porosity is underestimated in a gas zone. Gas is expandable so less gas volume can fill larger pore space, which leads to less amount of hydrogen compared to fluids filling the same pore. The neutron log response depends on the detector type, distance from source and detector, and lithology (17). Because of the high sensitivity of hydrogen, the neutron device measures porosity which can read directly from the neutron log without any derivation or calculation (18).

4.4.3. Sonic Log. The sonic log is an active tool and is one of the porosity logs that measures interval transit time of primary sound wave travelling to the formation. Lithology, porosity, and fluids in the pore spaces all affect the sonic transit time. The applications of sonic log are porosity determination, rock properties determination, formation stress determination, abnormal pressure detection, and fracture detection (17).

4.5. RESISTIVITY LOG

The resistivity log is an active tool that is used to detect water bearing zones versus hydrocarbon zones, indicate permeability, and define resistivity porosity. The most important aim for resistivity log is to detect water bearing zones. If formation water resistivity, porosity, true formation resistivity, cementation factor, tortuosity factor, and saturation exponent are known water saturation can be derived from the Archie equation (17). A resistivity from least to greatest is the following: salt

water, fresh water, oil, gas, and rock. Three types of resistivity logs can be used for hydrocarbon detection: deep resistivity, medium resistivity, and shallow resistivity. Shallow resistivity is in the flushed zone, medium resistivity is in the invaded zone, and deep resistivity is in the uninvaded zone. Before doing hydrocarbon interpretation, all of these parameters must be corrected using an appropriate tornado chart. Figure 4.1 shows that the resistivity increases linearly with the borehole distance. This increasing is a strong sign for hydrocarbon zones because hydrocarbons are more resistive than formation water. Figure 4.2 represents that resistivity decreases with borehole distance and deep resistivity is close to formation water resistivity. This shows that no hydrocarbon in the the formation.

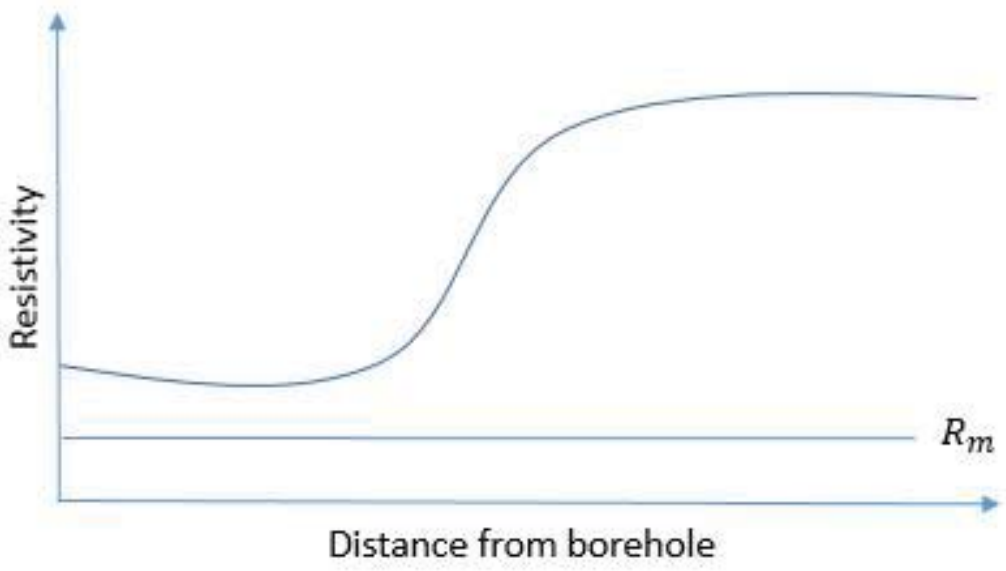

Figure 4.1: Resistivity Profile in Hydrocarbon Formation

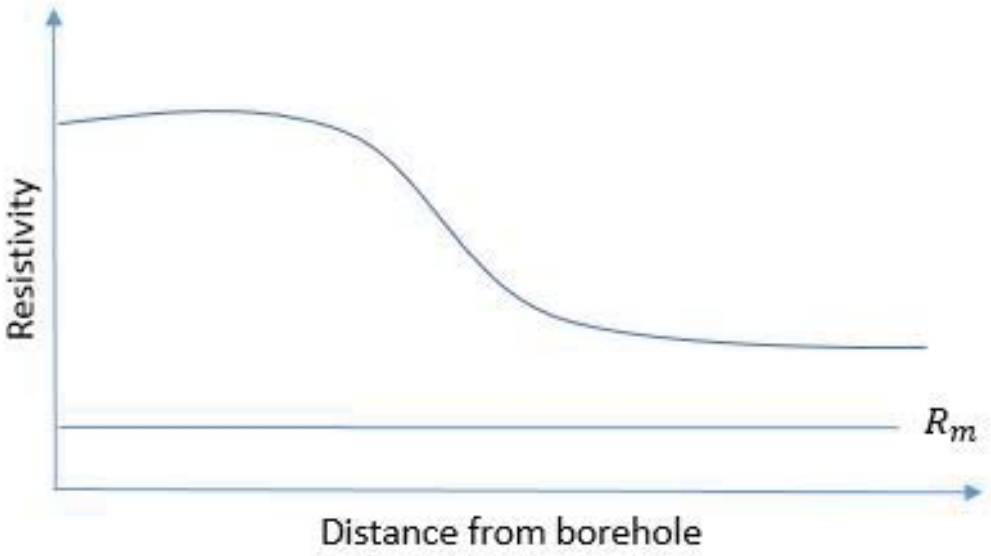

Figure 4.2: Resistivity Profile in Nonhydrocarbon Formation

5. PETROPHYSICAL ANALYSIS

5.1. FACIES ANALYSIS

Defining lithofacies is crucial for property modeling because all of the petrophysical parameters, such as porosity and permeability depend on facies type. In addition, fluid saturations directly depend on the facies type (19). In this study, core data and log data were available for facies analysis of the formation. In the reservoir area, core data and log data were available from five different wells. Using only core data or log data has many disadvantages. Core data is not available for the complete depth of the formation and the formation is heterogeneous, so using only core data is not accurate. However, log data is affected by many factors such as hole conditions such as oversize hole and different types of mud usage, so calibration of the log data and core data is very important to get the most accurate facies analysis for the formation (20). The facies type, which mostly differentiates between sandstone and shale, or limestone and dolomite provides a knowledge of reservoir quality. Correlation of the logs (this study uses gamma ray, spontaneous potential, caliper, and porosity logs) and core data give the most accurate qualitative information like facies type and quantitive information such as grain size, matrix density and bulk density in formation.

Crossplots are used to define lithology and petrophysical parameters using different types of logs. Many types of crossplots are available for different outputs. In this study, these types of crossplots were used:

Density log measures electron density, and from this, bulk density can be directly obtained. Neutron log measures hydrogen content in the formation, and it directly gives the porosity value of the formation. Further, gamma ray log measures

natural radioactivity of the formation, and it gives information about shale or non –shale formations. Because shale mostly has clay minerals and clay has high radioactivity, shaly formations have high gamma ray values. Density –neutron –gamma ray crossplots give an indication about lithology and porosity of the formation (21). In this study, this type of crossplot was used for each well.

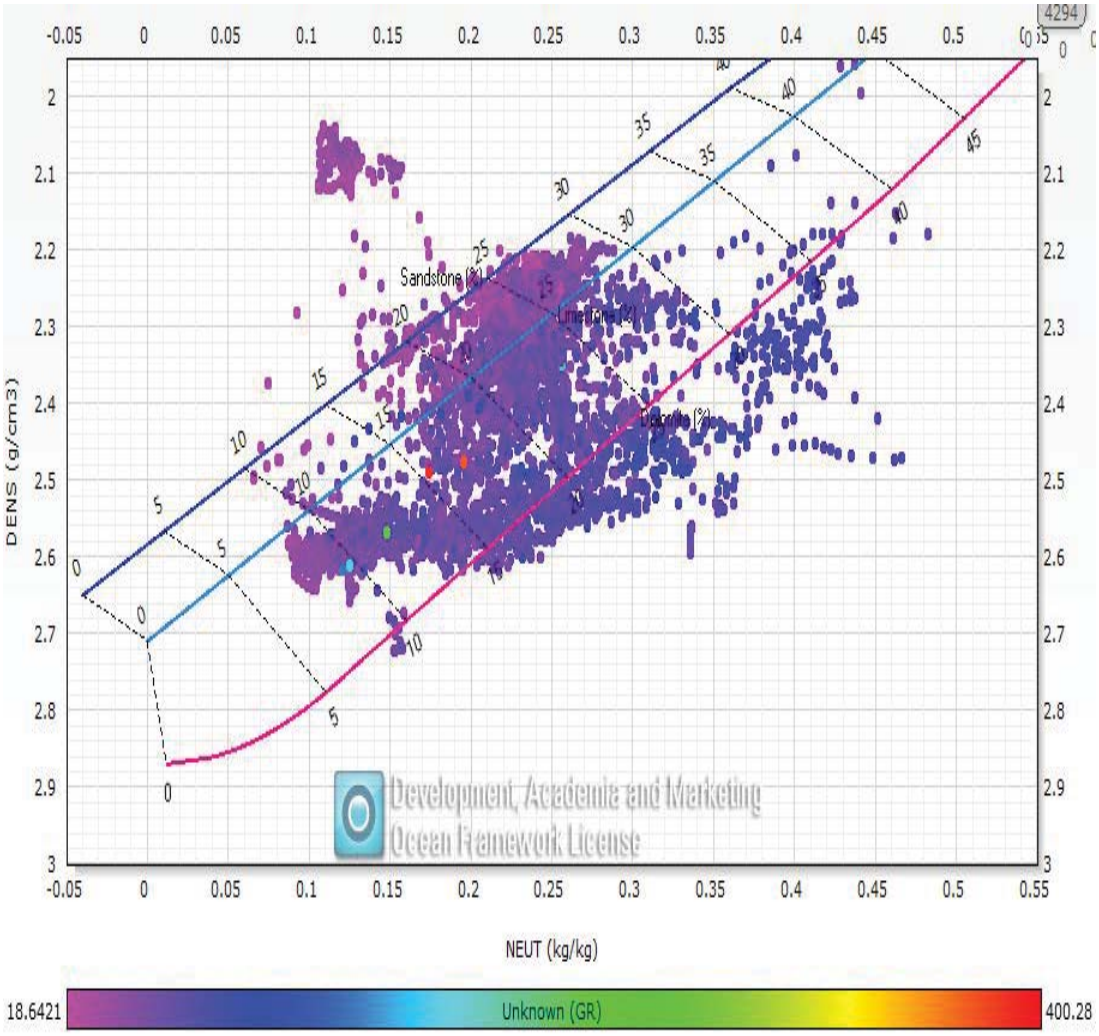

Figure 5.1: Density-Neutron-Gamma Ray Crossplot in Maui-1 Well

The Maui-1 well crossplot in Figure 5.1 that porosity range is 15% to 27% and also it shows that gamma ray value of the formation mostly is low so, this proves formation contains mostly porous sandstone.

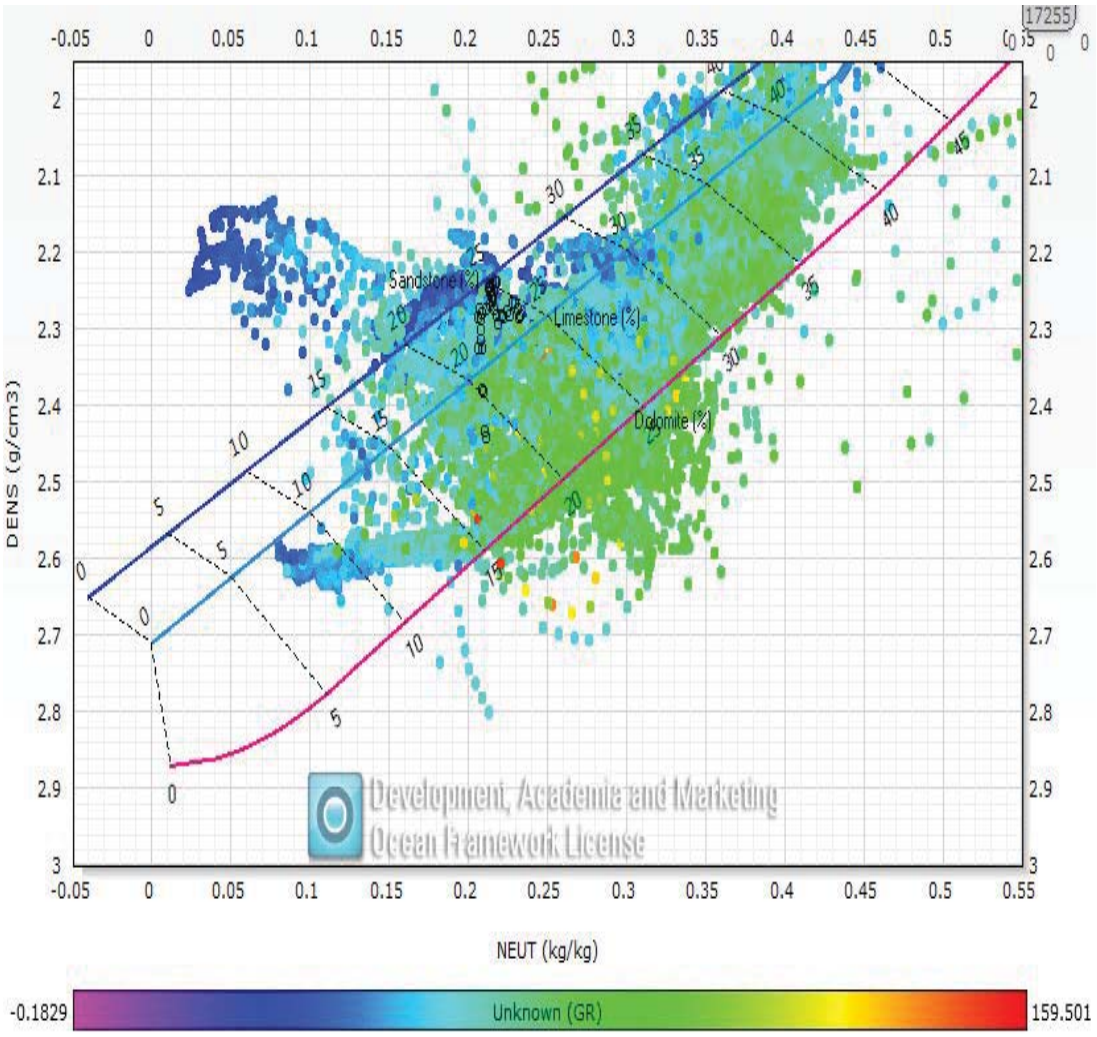

Figure 5.2: Density-Neutron-Gamma Ray Crossplot in Maui-7 Well

The Maui-7 well crossplot in Figure 5.2 shows that the porosity range is 18% to 40% and also it shows that gamma ray value of the formation mostly is low so, this proves formation contains mostly highly porous sandstone.

The MB-P(8) well crossplot in Figure 5.3 shows that the porosity range is 12% to 24% and also it shows that gamma ray value of the formation mostly is low so, this proves formation contains mostly porous sandstone.

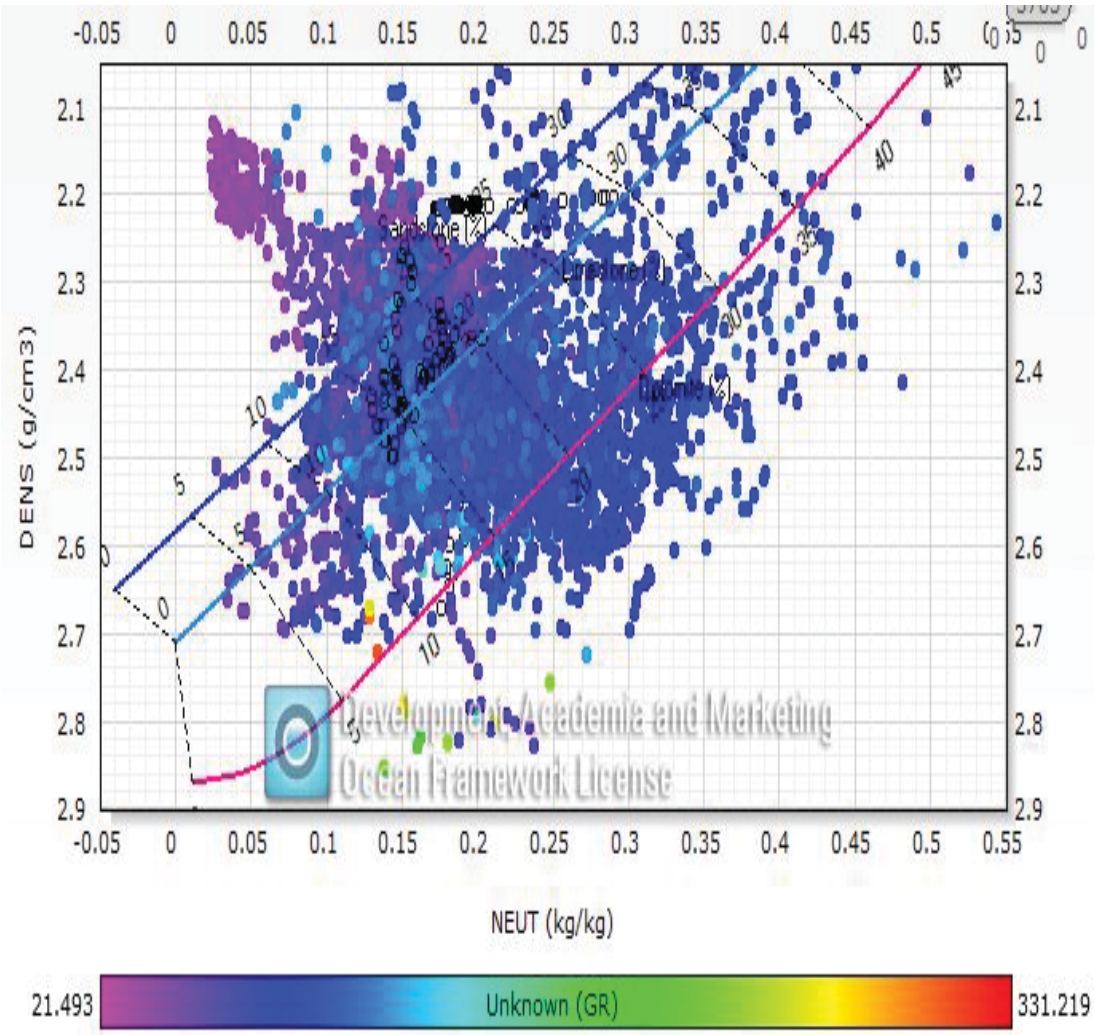

Figure 5.3: Density-Neutron-Gamma Ray Crossplot in MB-P(8) Well

The MB-R(1) well crossplot in Figure 5.4 shows that the porosity range is 15% to 23% and also it shows that gamma ray value of the formation mostly is low so, this proves formation contains mostly porous sandstone.

The MB-W(2) well crossplot in Figure 5.5 shows that the porosity range is 16% to 24% and also it shows that gamma ray value of the formation mostly is low so, this proves formation contains mostly porous sandstone.

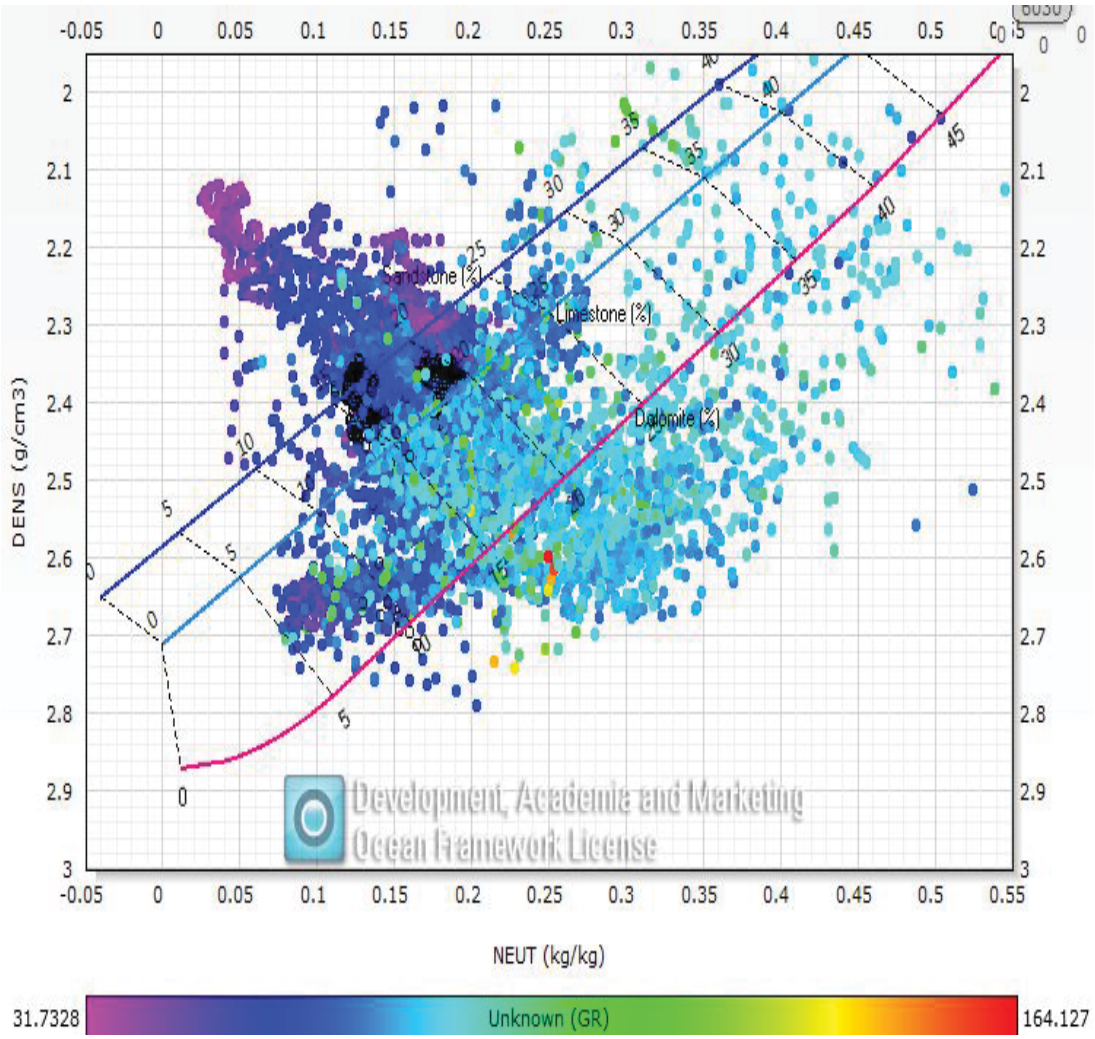

Figure 5.4: Density-Neutron-Gamma Ray Crossplot in MB-R(1) Well

5.2. POROSITY

Porosity is the pore volume percentage to bulk volume. Porosity can be calculated with different tools, such as from core data and well log data. Three types of logs, density log, neutron log, sonic log can be directly used for the porosity calculation in addition to other logs that can also be used to estimate porosity such as resistivity logs.

5.2.1. Porosity Calculation using Core Data. Porosity can be calculated from lab experiments, and this is the most accurate way to obtain the actual porosity

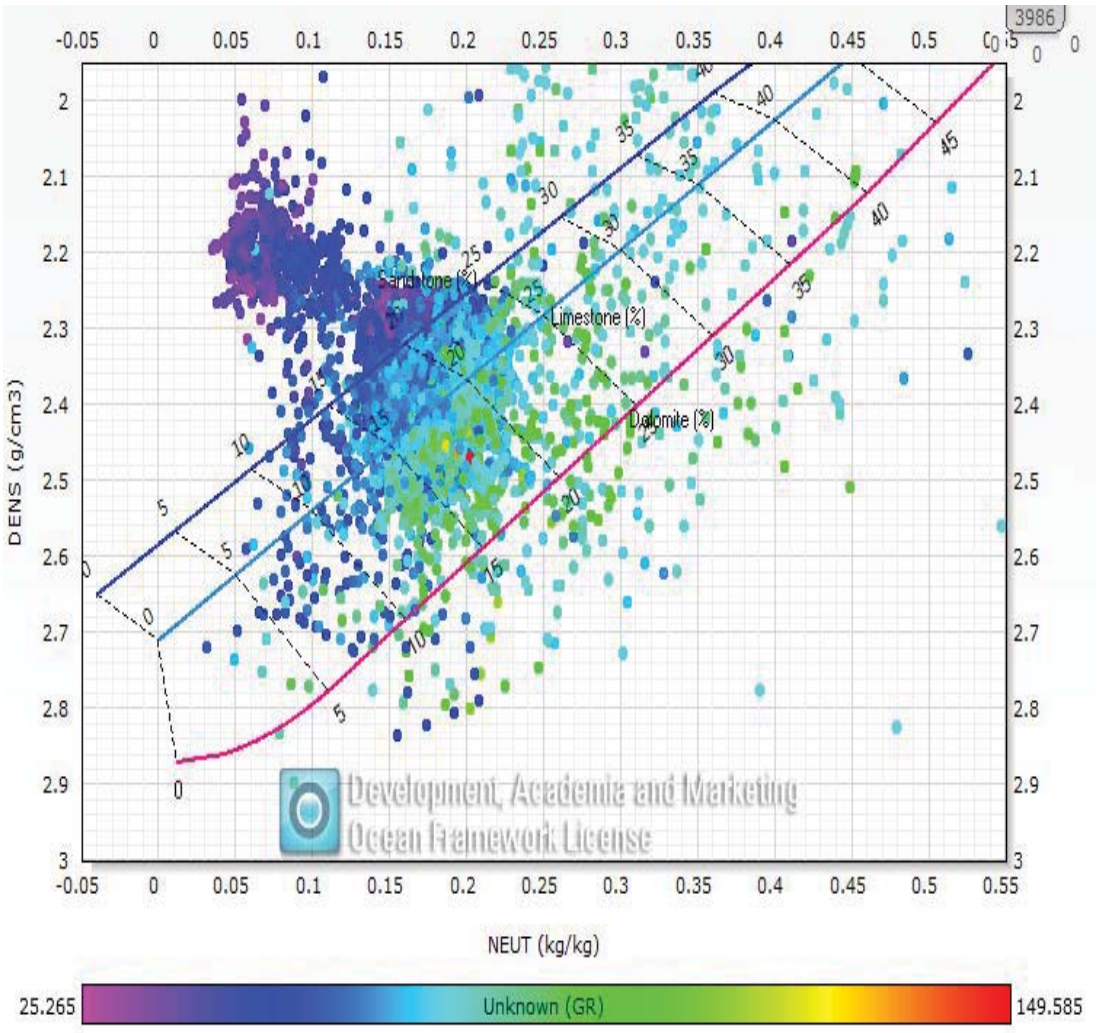

Figure 5.5: Density-Neutron-Gamma Ray Crossplot in MB-W(2) Well

value because the core data is an exact sample from drilling. Core data is available for this study with limited depth range, so porosity was first calculated from porosity logs, then calibrated from the core data where core data is available and the most accurate result was obtained. In reservoir zones, the porosity range is 17 to 35%, indicating that the formation is highly porous.

5.2.2. Porosity Calculation using Well Log Data. Three diferent types of well logs including density logs, neutron logs, and sonic logs are used to calculate porosity.

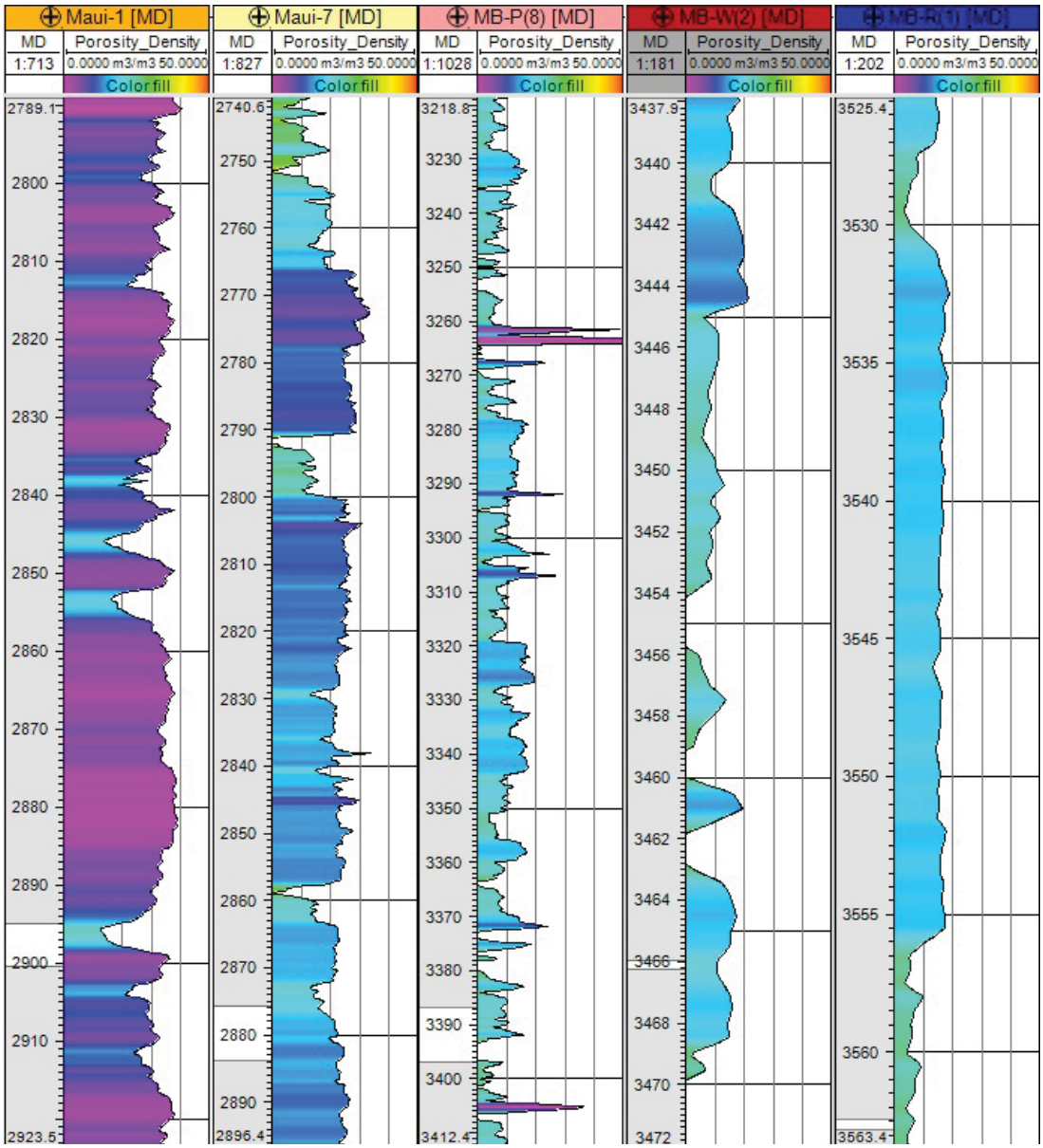

Figure 5.6: Porosity Measurement from Core Data by Lab Experiment

Density log directly gives a value of bulk density. Bulk density and porosity have a direct relationship. This formula is used commonly to show the relationship between bulk density and porosity:

$$\rho_b = \rho_f \phi + \rho_{ma}(1 - \rho) \tag{5.1}$$

where,

ρ_b: bulk density which includes both fluid and rock,

ρ_f: density of the saturating fluid,

ρ_{ma}: density of the rock matrix,

ϕ: porosity.

In gas zones, the density porosity is overestimated because gas has lower density than other fluids, which minimizes the matrix density and therefore increases the estimated porosity.

Porosity can be directly read from neutron logs. After the porosity is read from neutron logs, the porosity must be corrected using density logs and charts. In gas zones, the porosity is underestimated in the neutron logs because a neutron tool detects on the amount of hydrogen existing in the formation, in gas zones porosity is underestimated because a lower amount of gas could occupy larger pore space and this leads to a lower amount of hydrogen, making the estimated porosity lower than the actual.

Porosity is computed from sonic logs by converting from interval transit time of primary waves to porosity. There are different ways to do this conversion. Each conversion depends on some factors, but the most important one is lithology. The first way to calculate porosity using sonic logs is the time average model. This model only valid if the lithology is homogeneously compacted, consolidated clean sandstones.

$$\phi = \frac{\Delta t - \Delta t_{ma}}{\Delta t_f - \Delta t_{ma}} \tag{5.2}$$

where,

Δt: Interval transit time,

Δt_{ma}: Interval transit time through the matrix,

Δt_f: Interval transit time through the saturating fluid.

The Wyllie equation can be use in consolidated sandstones and carbonates to calculate porosity from sonic log.

$$\phi_{sonic} = (\frac{\Delta t_{log} - \Delta t_{ma}}{\Delta t_f - \Delta t_{ma}}) * \frac{1}{C_p} \tag{5.3}$$

where,

Δt_{log}: Interval transit time from the log,

Δt_{ma}: Interval transit time through the matrix,

Δt_f: Interval transit time through the fluid,

C_p: Compaction factor.

The Raymer–Hunt–Gardner (RHG) equation is used to calculate porosity from sonic logs for any lithology samples. Because of that, RHG method is the most usable method to calculate porosity from sonic logs.

$$\rho_{sonic} = \frac{5}{8} * \frac{\Delta t_{log} - \Delta t_{ma}}{\Delta t_{log}} \tag{5.4}$$

Δt_{log}: Interval transit time from the log,

Δt_{ma}: Interval transit time through the matrix

To correct sonic porosity, the hydrocarbon effect must be considered because hydrocarbons increase interval transit time. Because of this, Hilchie improved a formula for oil and gas hydrocarbons.

For gas: $\phi = \phi_{sonic} * 0.7$

For oil: $\phi = \phi_{sonic} * 0.8$

Obtaining porosity with only one measurement is not as accurate because many factors affect the measurement of porosity from log data, so porosity calculations need to be corrected by using at least two different tools. Single measurement

tools of porosity are density logs, neutron logs, and sonic logs. The most common two tools measurements are (21):

- Neutron and density logs
- Neutron and sonic logs
- Spectral density

Three different porosity measurement tools are:

- Mineral Identification (MID) Plots
- Neutron, Density, and Sonic Logs
- Neutron and Spectral Density Logs

In this study, different types of log data are used and calibrated with core data to obtain the most accurate results. For reservoir engineers, the effective porosity is more important because pores must be connected in order that fluid may flow, so after total porosity is calculated the shale effect is considered and effective porosity is calculated. Figure 5.7 shows that porosity calculated from density log and the results are close to the core data results.

5.3. PERMEABILITY

Permeability is the ability of the rock layer to transmit fluids (22). The unit of the permeability is darcy (d) or this unit can be converted to the millidarcy (mD). Permeability knowledge is important to describe a reservoir. In addition, it helps with effective completion designs, successful water injection programs, tertiary recovery, and reservoir management (23). Henry Darcy found an equation about basis of permeability (24).

$$q = \frac{KA\Delta p}{\mu L} \tag{5.5}$$

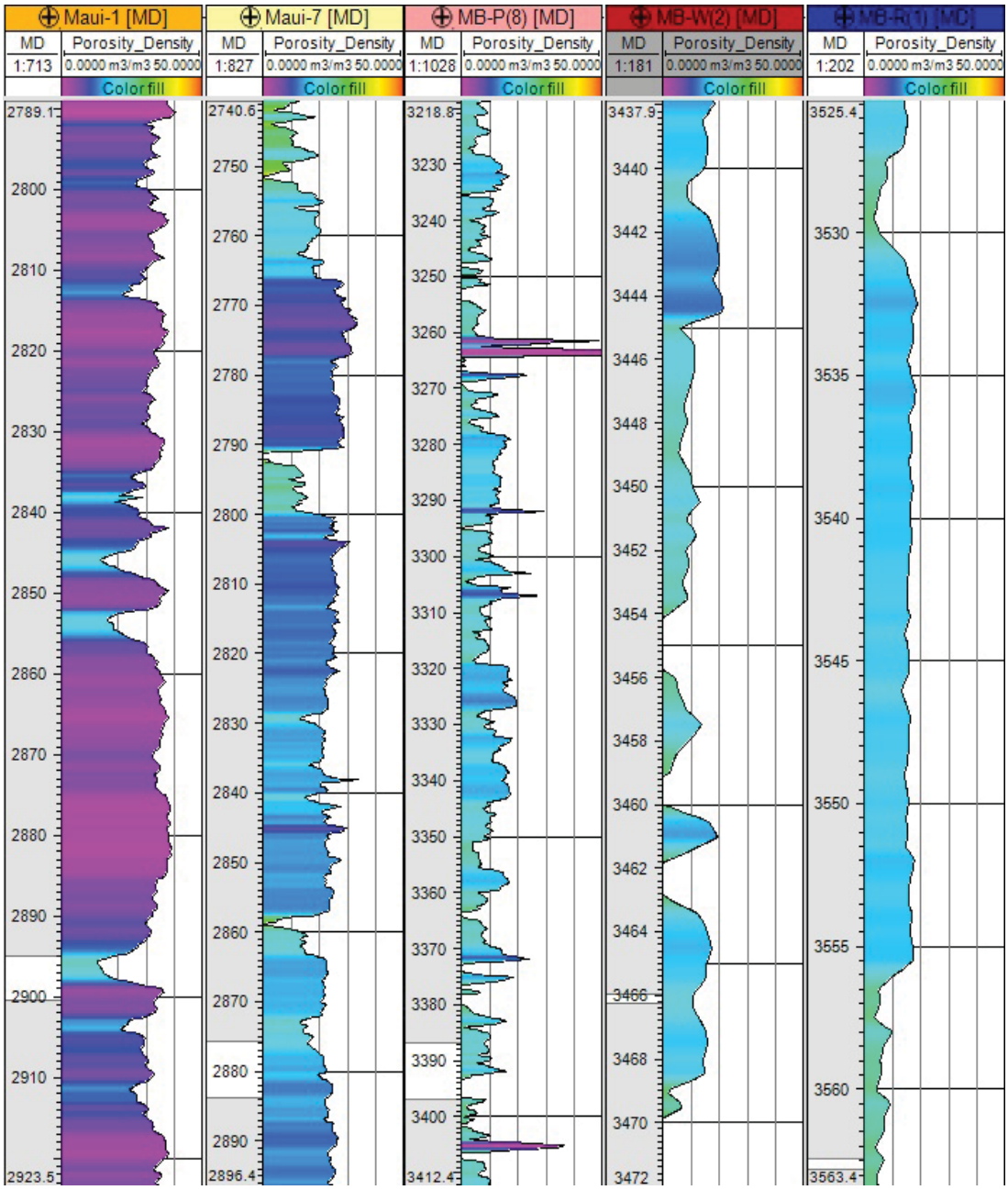

Figure 5.7: Porosity Calculation using Density Log

where,

q= water flow rate $[cm^3/s]$,

K= constant of proportionally that is characteristic of the sand pack [Darcy],

A= cross-sectional area of the sand pack $[cm^2]$,

Δp= total pressure drop $[atm]$,

μ= viscosity $[cP]$,

L= length $[cm]$.

Permeability can be calculated both from core data and log data. Permeability values from core data is the most accurate; however, if it is not available, log data can be used for high permeable formations. The formula, which was built from Wyllie-Rose (1950) to calculate permeability for high permeable formations, is

$$K = \frac{62500 * \phi_e^6}{Sw_{irreducible}^2} \tag{5.6}$$

where,

K= permeability $[mD]$,

ϕ_e= effective porosity,

$Sw_{irreducible}$ = irreducible water saturation.

In this research, core data was available, so permeability was calculated from the formula, which was built from Wyllie-Rose using porosity and irreducible water saturation. Then, it was calibrated with the core data to obtain the most accurate permeability range for the study area. Figure 5.8 shows that permeability ranges from core data and in reservoir zones permeability range is 300 to 3700 mD.

5.4. WATER SATURATION

Water saturation can be defined as the ratio of water volume to pore volume. It is calculated by effective porosity and resistivity logs. Determining water saturation is crucial because hydrocarbon saturation can be calculated from water saturation (25). Water saturation in uninvaded zones can be calculated from the Archie equation.

$$Sw^n = \frac{R_w}{\phi^m * R_t} \tag{5.7}$$

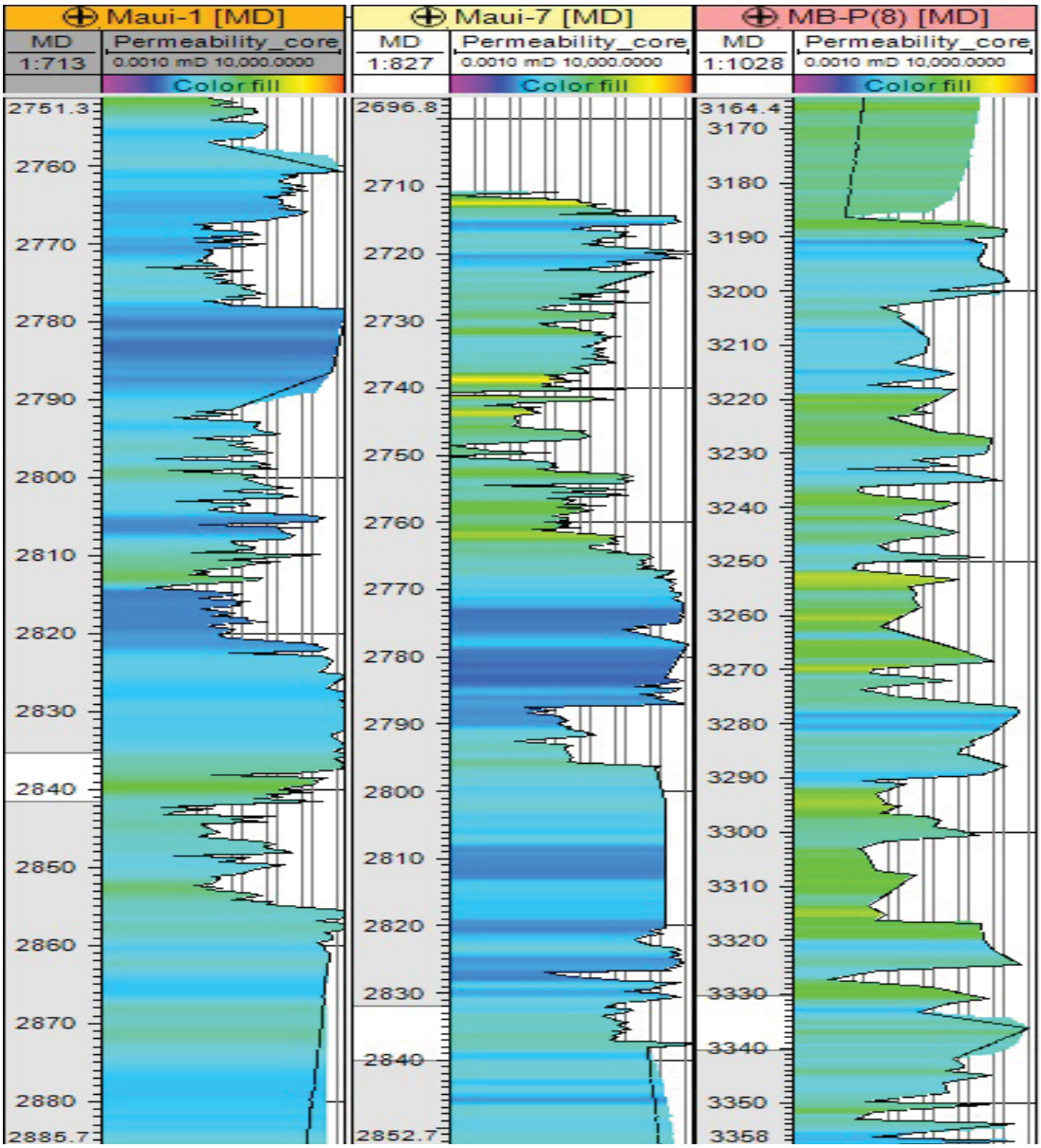

Figure 5.8: Permeability Calculation using Core Data

where,

Sw= water saturation of the uninvaded zone,

n= saturation exponent,

R_w= formation water resistivity at formation temperature,

ϕ= porosity,

m= cementation exponent,

R_t= true formation resistivity.

In addition, permeability calculation depends on irreducible water saturation if core data is not available. Irreducible water saturation indicates oil volume and producible water from reservoir. Irreducible water saturation also influences the reservoir production rate. It also needs to be known to calculate original oil in place (OOIP). In this study water saturation has been calculated using logging tools and used for hydrocarbon saturation and original oil in place calculations.

5.5. SHALE VOLUME

Knowledge of shale volume is crucial because it helps to calculate formation porosity, fluid content, and overall rock quality. The vast portion of shale is made up of clay minerals, but clay minerals occur in other rocks. Most of the logging tools are affected by shale content in a formation, so knowledge of the clay content is very important to obtain accurate formation evaluation. Many tools can be used to determine volume of shale, both single tools like spontaneous potential, gamma ray, neutron, and resistivity and combination of two indicators like neutron-density and neutron-acoustic. None of these indicators give an accurate result for the amount of shale; however, each indicator is calibrated for different situations (26). The shale effect decreases the magnitude of spontaneous potential log. Clay minerals increase radioactivity, and since gamma ray logs read radioactive minerals, their readings are affected by clays .The amount of clay decreases the resistivity because clay is a conductive mineral. In addition, all of the porosity logs (density, neutron, and sonic) are affected by the volume of shale. Neutron logs are overestimated in porosity reading in shale formations; however, density logs are underestimated in porosity reading. Furthermore, the amount of shale increases the interval sonic travel time.

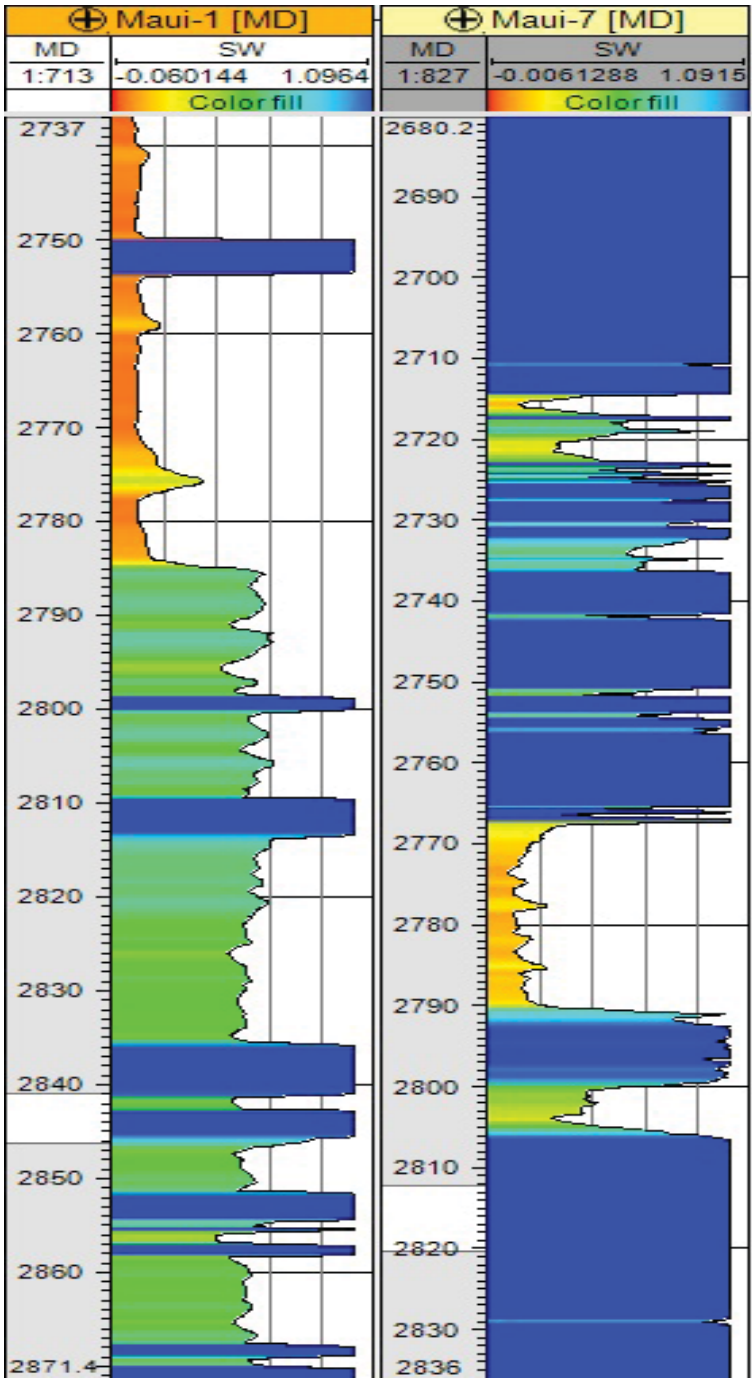

Figure 5.9: Water Saturation Calculation using Archie's Equation

The implications of shale effects are that shale reduces resistivity contrast between formation fluids, reduces water saturation, and if shale volume is overestimated a water zone can appear like a hydrocarbon zone. To get hydrocarbon from pores,

effective porosity needs to be calculated instead of total porosity, and shale volume must be known to calculate effective porosity. The shale volume formula is

$$\phi_t = V_{sh}\phi_{sh} + \phi_e \tag{5.8}$$

where,

ϕ_t= total porosity,

V_s= shale volume,

ϕ_{sh}= shale porosity,

ϕ_e= effective porosity.

The volume of shale formula can be written as the following (27):

$$V_{sh} = \frac{\phi_t - \phi_e}{\phi_{sh}} \tag{5.9}$$

where,

V_{sh}= shale volume,

ϕ_t= total porosity,

ϕ_e:=effective porosity.

The volume of shale also can be calculated from the formula (21):

$$V_{sh} = \frac{(GR_{log} - GR_{clean})}{(GR_{sh} - GR_{clean})} \tag{5.10}$$

where,

GR_{log}= gamma ray value at the specified depth,

GR_{clean}= gamma ray value at a clean formation baseline,

GR_{sh}= gamma ray value at a shale baseline.

According to the shale volume, formation can be classified as a clean formation if $V_{sh} < \%10$, it can be classified if $10\% < V_{sh} < \%33$ as a shaly formation, and it can be classified as a shale formation if $V_{sh} > \%33$ (27).

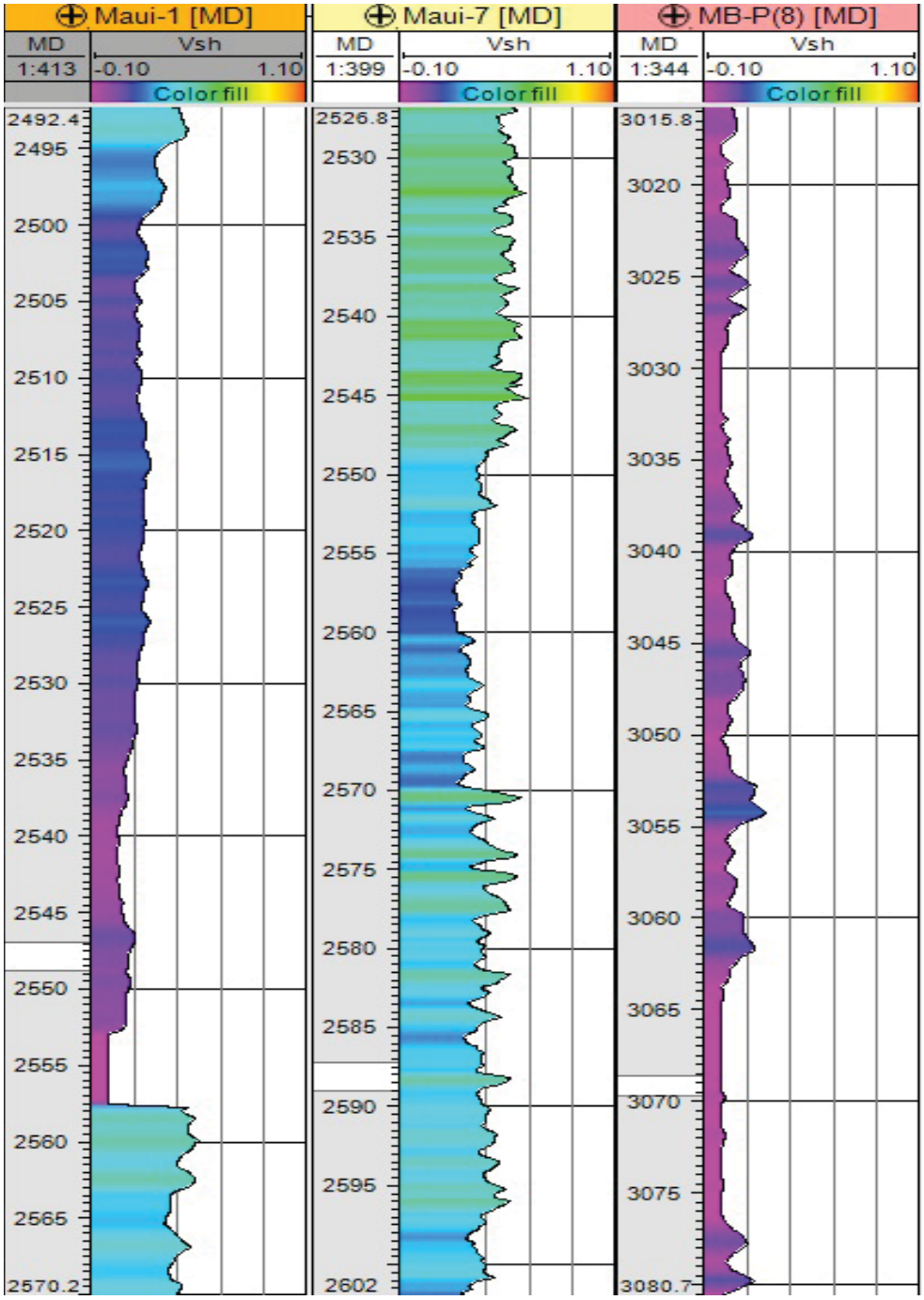

Figure 5.10: Shale Volume Calculation using Gamma Ray Log

5.6. NET–TO–GROSS RATIO

It is very important to determine net pay thickness to calculate original hydrocarbon in place, and this factor strongly affects hydrocarbon in place calculation, total energy balance of the reservoir, and recovery processes (28). All of the petrophysical parameters that have been calculated are inputs of net-to-gross ratio. Net pay thickness is the most important factor to calculate hydrocarbon in place calculations because it affects the reservoir management, and further total energy balance calculation gives an estimation for movable and nonmovable hydrocarbon volume. In addition, net pay determination is a crucial factor to estimate potential hydrocarbon availability for secondary recovery. Secondary recovery processes are very important because without these only 15% to 25% of hydrocarbon can be recovered; however, using secondary recovery techniques, this percentage can be improved up to 40% or higher. We cannot get 100 percent recovery because of residual oil, high oil viscosity, heterogeneity, fractures, and oil wet rock factors. Cutoffs, which are upper and lower limits of parameters are used to convert from gross thickness to net pay thickness. Gross thickness is a thickness that is from top of the reservoir to base of the reservoir. Gross thickness includes both reservoir rocks and nonreservoir rocks. After applying the shale volume cutoff, which eliminates the portion of the formation that contains large quantities of shale, gross sand thickness, which includes only reservoir rocks, can be defined. Next the applied porosity cutoff, which eliminates a portion of the formation(low porosity), is applied to determine net sand thickness, which is the fraction of the gross sand that is porous, permeable, and contains water and hydrocarbons. Finally, the water saturation cutoff is applied, which eliminates the portion of the formation that contains a large volume of water in the pore space. the final result after these cutoffs is net pay (29).

5.7. RESERVE ESTIMATION

After calculating all of the petrophysical parameters, hydrocarbon in place can be calculated and reserve estimation can be determined. To get all of these estimations, economical decisions can be determined from the current hydrocarbon price. Oil in reservoir can be calculated by the formula:

$$N = \frac{7758A}{B_0} \sum_{i=1}^{n} h\phi(1 - S_w) \tag{5.11}$$

where,

N= oil in place (stb),

A= drainage area (acres),

B_o= formation volume factor (rb/stb),

h= net pay thickness (ft),

ϕ= porosity,

S_w= water saturation.

Gas in reservoir can be calculated by the formula:

$$G = \frac{43560A}{B_g} \sum_{i=1}^{n} h\phi(1 - S_w) \tag{5.12}$$

where,

G= free gas reserve (scf),

A= drainage area (acres),

B_g= gas formation volume factor (rcf/scf),

h= net pay thickness (ft),

ϕ=porosity,

S_w= water saturation.

Reserve defines as a

$$R = N \times E \tag{5.13}$$

where,

R= reserves,

N= oil in place or free gas reserve,

E= recovery factor.

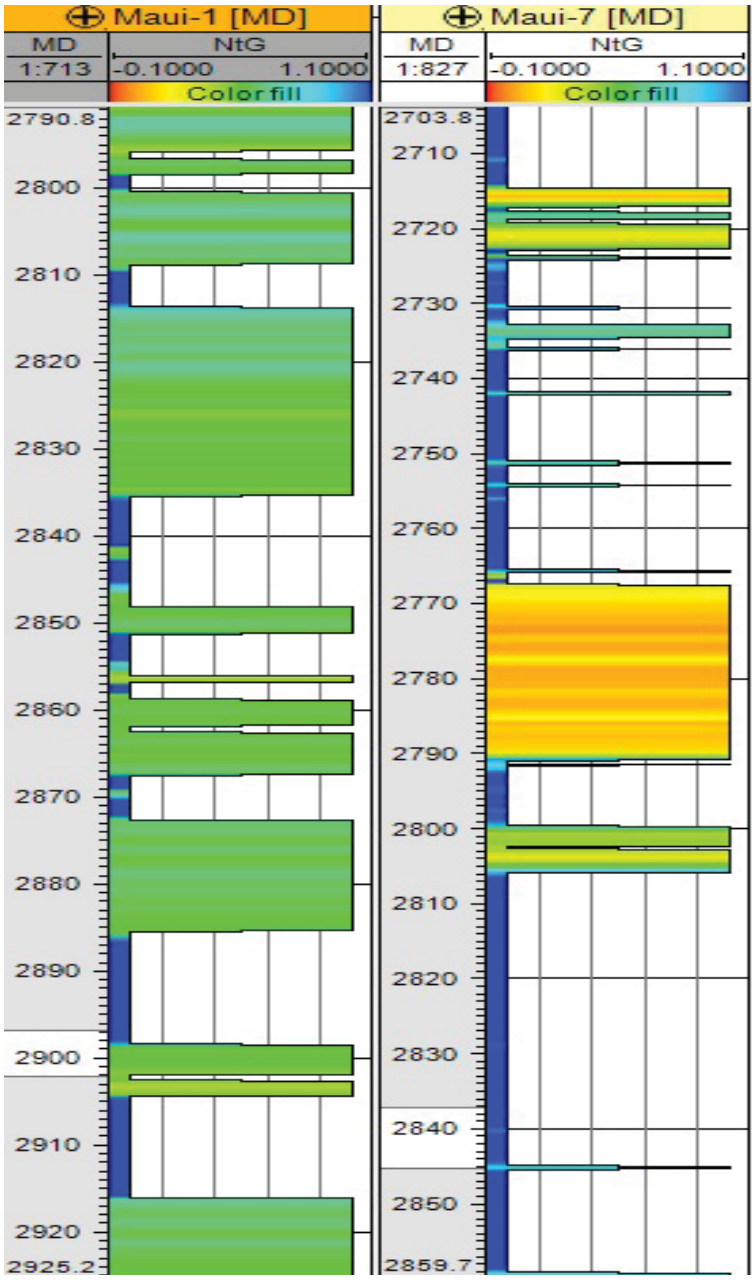

Figure 5.11: Net-to-Gross Ratio Calculation using Cutoffs

6. 3D PROPERTY MODELING

6.1. WELL LOG UPSCALING

Upscaling, or homogenization, is a process of averaging static and dynamic characteristics of the model and it assigns all of the coarse grid cells (30). Upscaling is an important step because each grid cell has a value; however, data from well log must be averaged, so upscaling is a necessary step for 3D modeling (31). The idea of upscaling is replacing the original value with the average value in both short length scale and long scale. The data come from experimental tests identified on core plug scale, but reservoir modeling and reservoir simulation software use gridblock scale, so the upscaling step must be done before going to modeling (32). There are many upscaling processes for different types of logs, such as discrete or continuous, and also for different parameters like porosity, permeability, and water saturation.

6.1.1. Discrete Logs Upscaling. This type of logs divided by lines to classify for different parameters. Each class has a different value; for example, sandstone is class 1, limestone is class 2, and shale is class 3 in facies log.

The best upscaling method for facies log is the "most of method", which applies the vast majority type of facies for each cell. For instance, if a cell has 55% limestone and 45% dolomite, the output is limestone because the vast portion of the formation is limestone. Unlike most of the petrophysical parameters, the facies log is divided by lines to define facies boundaries. In this study, five wells that had already created facies log using core and well log data were upscaled using the "most of" averaging method. After upscaling the formation mostly has sandstone, siltstone, and claystone. In addition, upscaled facies are essential because they affect all of the

petrophysical parameter calculations. Because of that, upscaled facies logs are used as a function of petrophysical parameters upscaling.

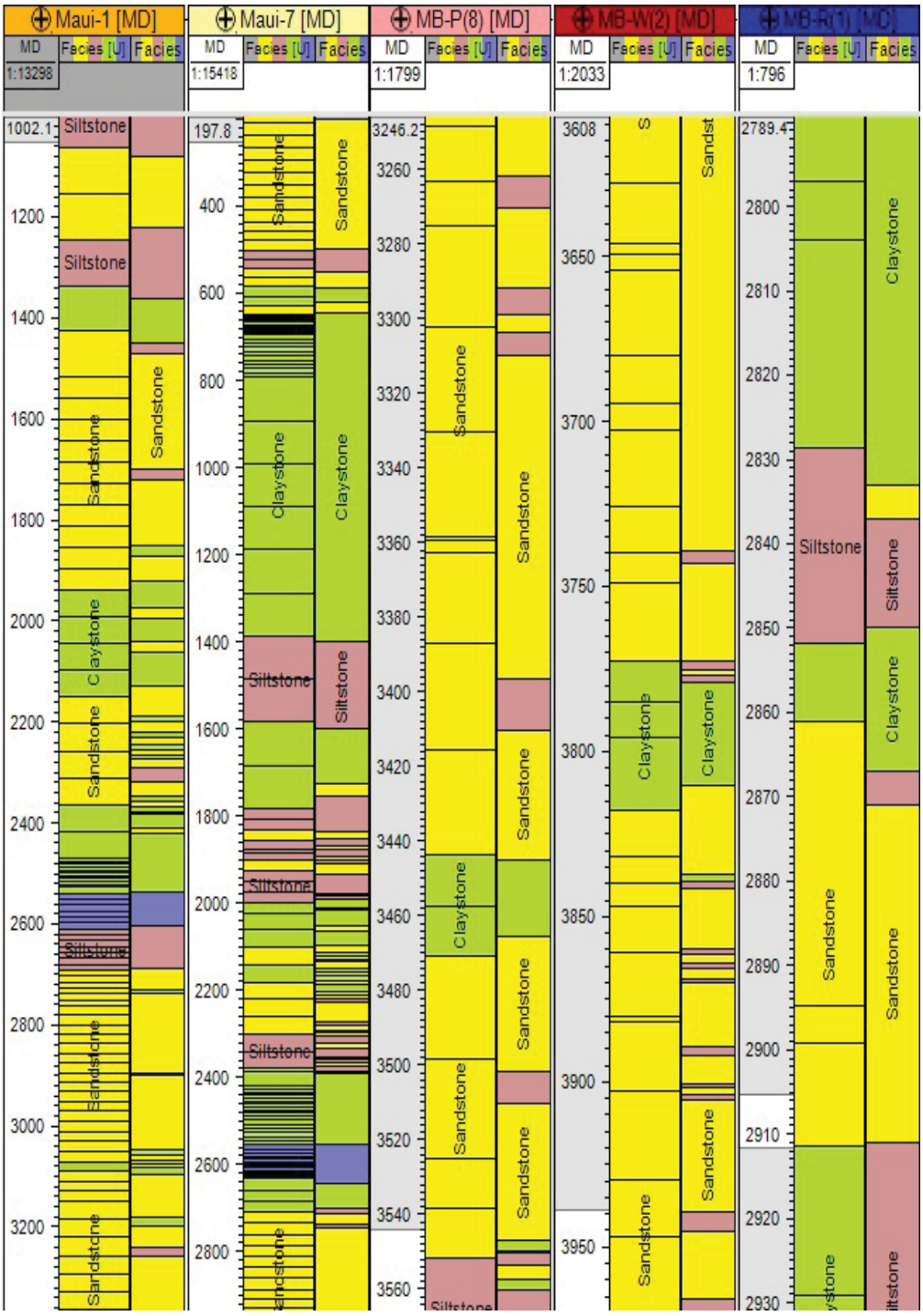

Figure 6.1: Upscaled Facies Logs in Five Different Wells in Maui-B Field

6.1.2. Continuous Logs Upscaling. The upscaling process for the continuous logs aims to get an average value for each cell (31). This step is essential because continuous logs are comprised of many points and each point has their own value, so modeling this log is very difficult. However, if the continuous logs are upscaled, there will be an average value for each cell, and modeling this log is much easier than the raw logs. There are many ways to use the upscaling process, and each way is convenient for different parameters, so before the upscaling process begins, the most suitable upscaling method for the parameter must be decided. In addition, different upscaling methods can be applied for each zone. This method is called the zone–specific averaging method. Continuous logs mostly bias with the discrete logs like facies. Thus petrophysical parameters can be matched with the lithology, and the results will be more clear. If facies data are not available or not very accurate, the weighting function can be used for upscaling process. Using the weighting function pore volume and fluid volumes can achieve the most accurate result.

For porosity upscaling, the arithmetic mean method was used in this study and upscaled facies log biased also to the continuous net–to–gross ratio log used as a weighting function in the arithmetic mean method. The arithmetic mean method formula is

$$X_a = \frac{1}{n}\sum_{i=1}^{n} X_i \tag{6.1}$$

For permeability upscaling, The harmonic method, arithmetic mean method, and geometric method were considered in this study, and the best method chosen for this study area was the harmonic method. The upscale process using the arithmetic method will not be accurate for permeability because the layers are not homogeneous in the study area. The harmonic method formula is

$$X_h = \frac{n}{\sum_{i=1}^{n} \frac{1}{X_i}} \tag{6.2}$$

For water saturation upscaling, the arithmetic mean method was used in this study to upscale water saturation, while water saturation upscaling, porosity and net–to–gross ratio logs are used as a weighting function.

Net–to–gross ratio upscaling was calculated by using arithmetic mean method. The arithmetic mean formula is

$$X_a = \frac{1}{n}\sum_{i=1}^{n} X_i \tag{6.3}$$

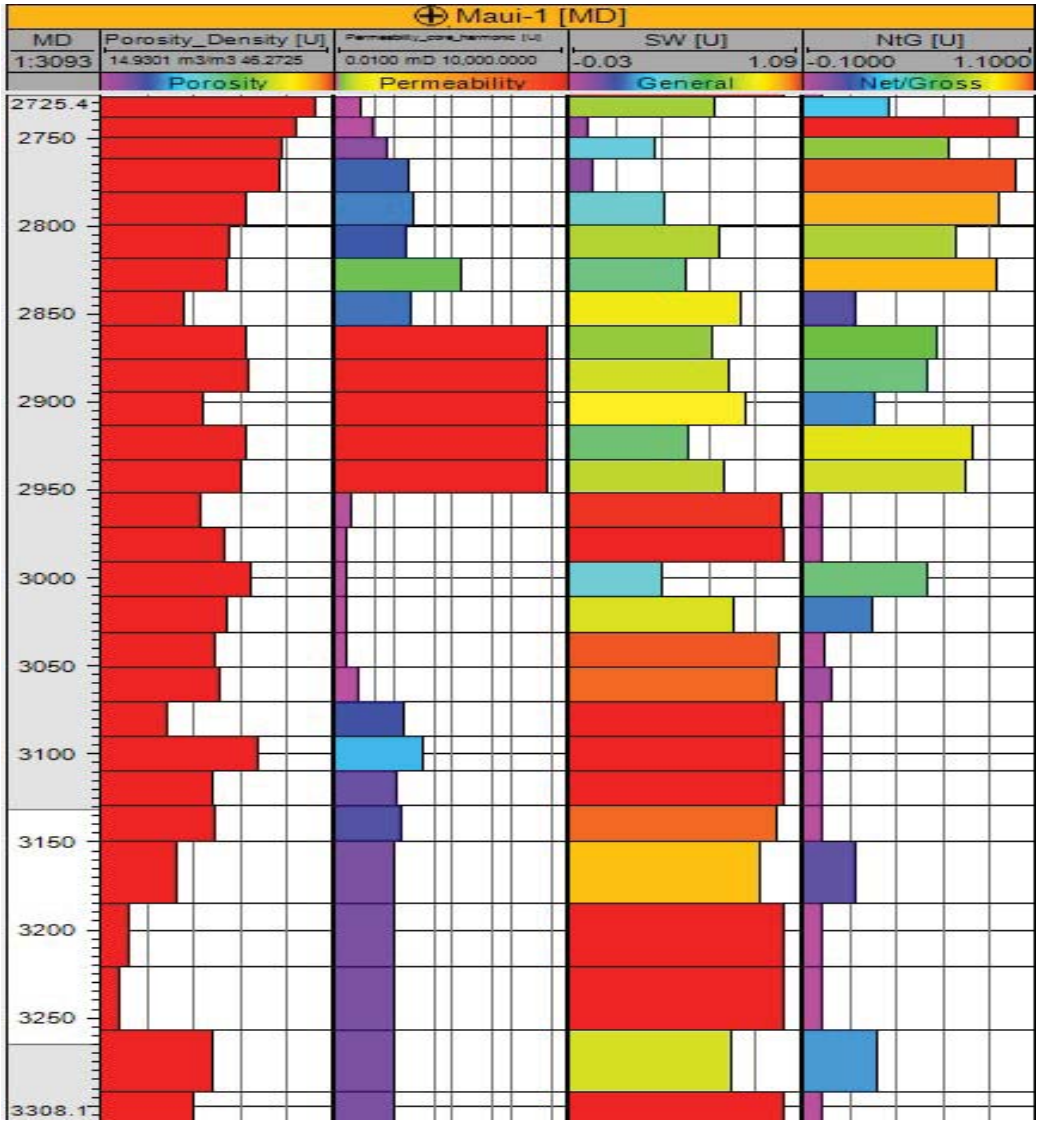

Figure 6.2: Upscaled Petrophysical Parameter Logs in Maui1 Well

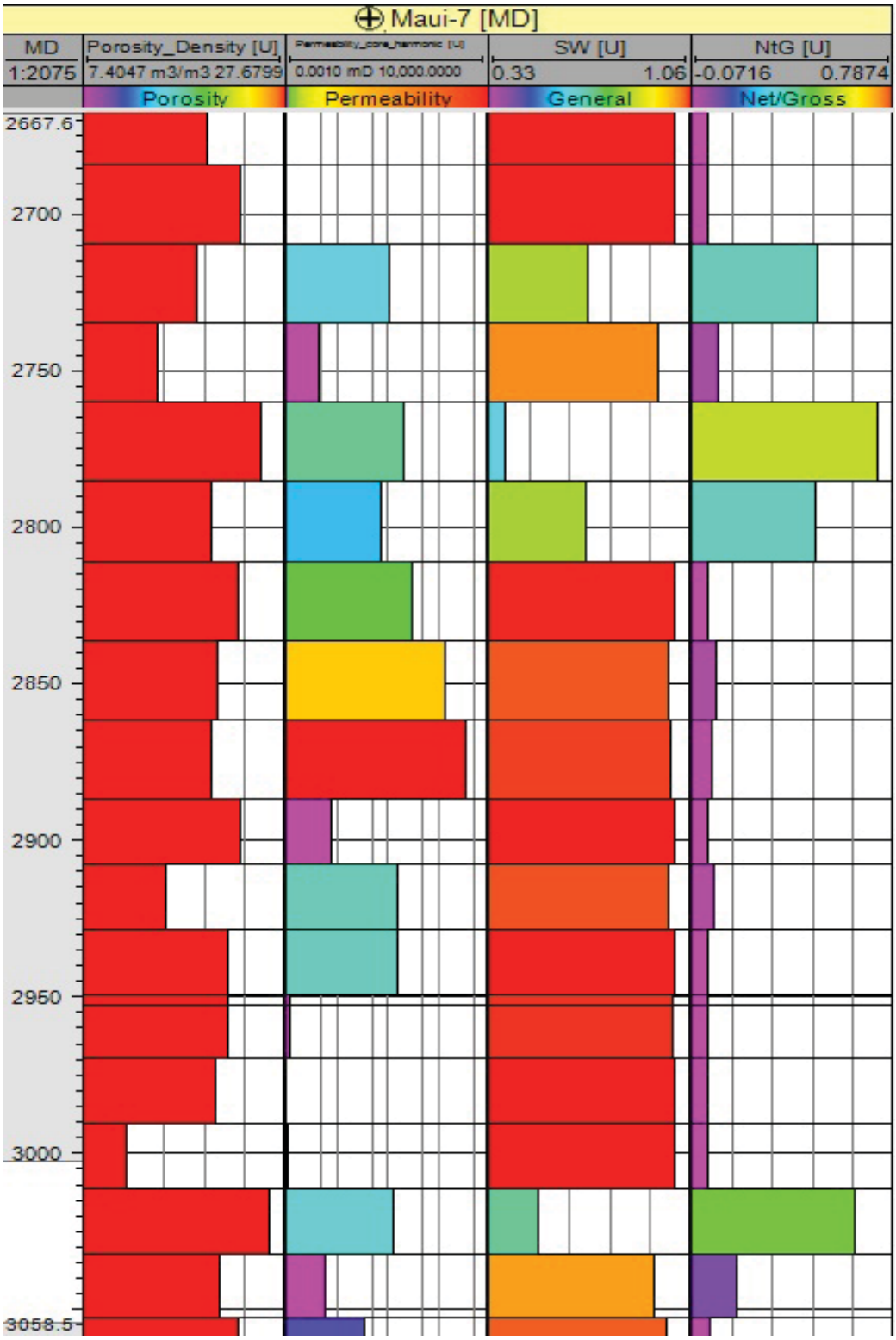

Figure 6.3: Upscaled Petrophysical Parameter Logs in Maui7 Well

6.2. GEOSTATISTICAL ANALYSIS

Statistics is a commonly used calculation method in different engineering and science areas. Histograms, charts, and tables assist to interpret the data, so statistics is a powerful tool for studies in petroleum engineering. Geostatistics is utilized to define spatial variability using statistics, mathematics, and geological-geophysical data. Geostatistics uses a probability function to predict properties of the formation. Geostatistics includes various tools and methods to calculate each property. Statistics and mathematics with geological-geophysical data are important to obtain accurate results for reservoir management, well locations, production, and recovery processes (33). The aim of using geostatistics tools is to obtain a prediction that suggests to produce hydrocarbons with the least work and highest profit using detailed 3D numerical property models. Geostatistics is a helpful tool to quantify reservoir heterogeneity. The geostatistics information will not be 100% accurate due to the uncertainties. There is no way to do facies analysis or petrophysical parameter analysis like porosity, permeability, and water saturation because wells are not located extremely close to each other and geological formations are not homogeneous so there will be an error in distribution analysis. This error is called uncertainty (19). Three basic statistical terms must be understood well for geostatistical analysis:

- **Probability:** Probability considers all of the parameters to obtain a value from 0 to 1. Many techniques are used to obtain an accurate probability value. It is very difficult to consider heterogeneous formation using the probability factor; however, if 3D models are run with possible different scenarios and then averaged for each cell, the result will be very accurate and close to the natural formation types or values for different parameters. In this study, each 3D model was run 1000 times after that calculated the arithmetic mean of each cell using the Monte Carlo simulation technique.

- **Variance:** Variance calculation is obtained by finding the mean value, then substracting this value from each value, squaring all of them, and finally averaging these square values. Low variance is much more accurate because it shows the values are close to each other and separation is low. In geostatistics, for example, if the formation is close to homogeneous like limestone, dolomite, or sandstone formation, the variance will be close to zero and statistical analysis will be easy. However, if the formation is heterogeneous like shaly sandstone and this formation has more than two types of lithofacies, the variance will be high and it will be more difficult to make a statistical analysis compared with the first situation.

- **Correlation:** Correlation is a method used to determine the relationship of different parameters. Correlation analysis is important because three different parameters are evaluated, so it gives an accurate prediction of reservoir and formation evaluation. The most common correlation type is porosity versus permeability with bias facies type for this analysis. After these basic calculations and before starting modeling distributions can be shown with histograms, which make a distribution visulation using graphics.

6.2.1. Variogram Analysis. Variograms are utilized to show spatial continuity and heterogeneity in the formation. Therefore, it is necessary to use this tool to obtain reliable results. Variograms show the nonsimilarity between two values based on the distance. In the variogram chart, the horizontal and vertical axes present the separation distance and the nonsimilarity of two values at the defined depth, respectively. Basically, variogram modeling is a powerful technique to define natural variations. Constitutively, variogram charts are used to define the nonsimilarity of related parameters with respect to the distance between two points. They are generated based on this nonsimilarity theory (34). Variogram analysis is vital for fluid flow

behavior in reservoir modeling due to the reservoir data limitation (35). Variogram analyses were performed using Petrel 2016 software.

6.2.2. Monte Carlo Simulation. Monte Carlo simulation is utilized to determine the uncertainties in the reservoir. The procedure of the simulation designs stochastic models and use a random number generator function and variance–reducing techniques. Monte Carlo simulation is used in many areas in petroleum engineering such as reservoir management, property calculations, hydrocarbon in place calculations, recovery processes, and petroleum economics. In this study, it was used to model facies of the formation and petrophysical parameters including porosity, permeability, water saturation, and net–to–gross ratio. In addition, the simulation was used to calculate hydrocarbon in place. The petrophysical parameters were upscaled and 3D models at each parameter were constructed with the probability function. They were averaged using the probability function. In this study, the number of iterations is set 1000, and arithmetic mean of the parameter was calculated. Furthermore, hydrocarbon in place calculations, which are both for oil and gas reservoirs, were completed by using the formula generated from Monte Carlo simulation.

6.3. 3D MODELING

Facies logs were created using core data and well log data after that the facies logs were upscaled with "most of method". Next, data analysis was done using variogram analyses to define heterogeneity of the formation. Then, the upscaled facies log was run 1000 times with sequential indicator simulation and lastly the arithmetic mean of each cell was calculated from these 1000 different 3D models using Monte Carlo simulation.

The three dimensional facies model was analyzed. Based on the analysis, the vast portion of the formation is sandstone and it represents with yellow color,

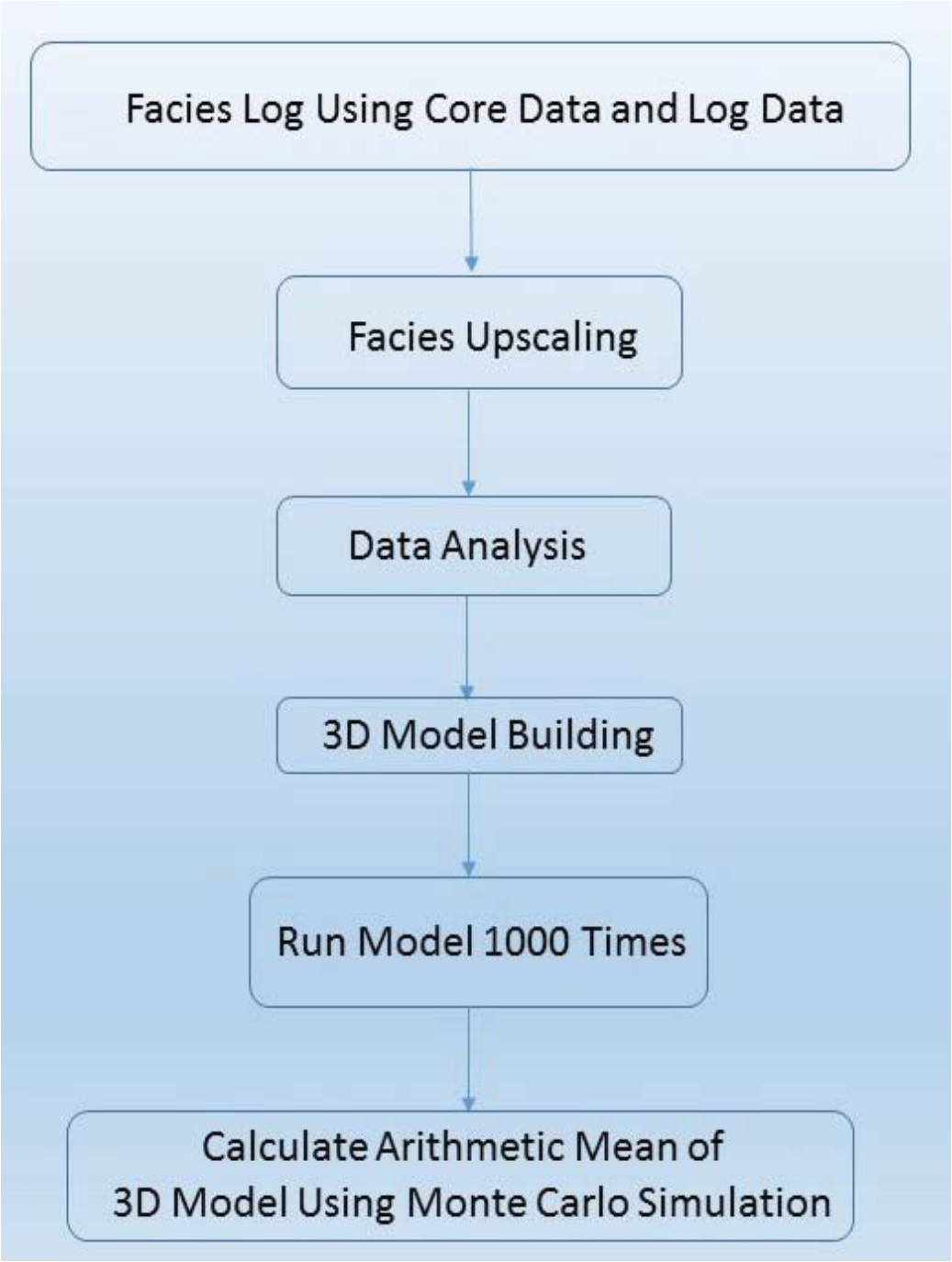

Figure 6.4: 3D Facies Log Workflow

the second majority of the formation rock is claystone and it is represented with turquoise color, next the green color represents sandstone/minor clay, lastly pink color represents limestone. Facies modeling is fairly significant for reservoir modeling

because the petrophysical properties are extremely related with the type of facies. The distribution of porosity and permeability is compelled by facies knowledge.

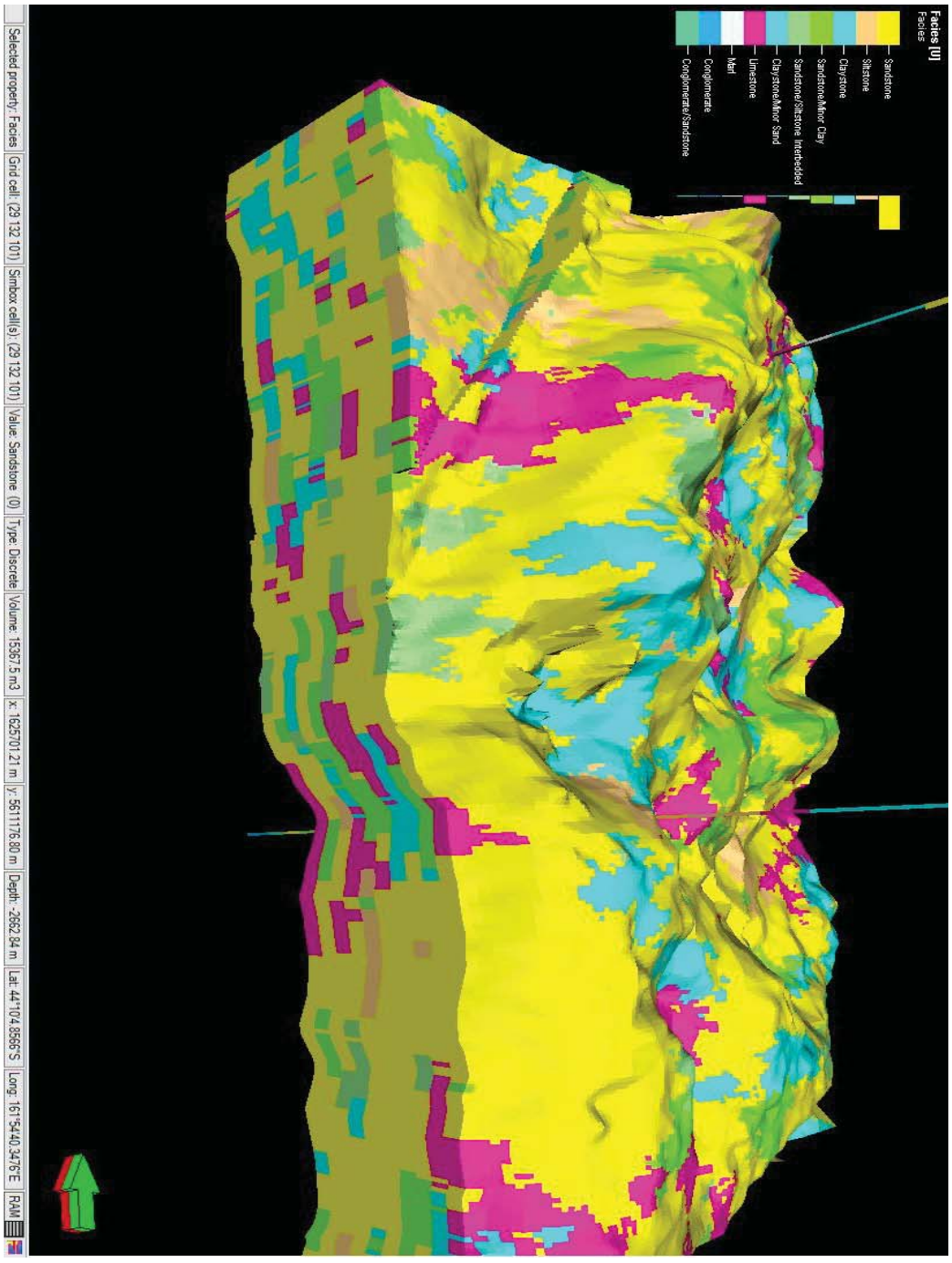

Figure 6.5: 3D Facies Model

Three dimensional petrophysical paramater calculations are extremely important for reservoir decisions because reservoir rock should be porous, permeable, hydrocarbon filled in the interconnected pores, and after cutoffs which are porosity, shale, and water saturation high net value. Porosity and permability are the main factors need to be considered in reservoir characterization and while considering these factors facies knowledge is vital because calibration of facies type and petrophysical parameter values provide high accuracy for reservoir decision.

Effective porosity is more important than total porosity because for hydrocarbon production interconnected pores are needed. In this study, effective porosity was calculated using total porosity and shale volume. The effective porosity range is 10%–15%. After considering effective porosity, permeability is also vital for reservoir decisions. In this study, core data and log data were calibrated to obtain permeability and in the reservoir area permeability was around 1000 mD. These two factors reveal that the reservoir area is both porous and permeable. Next, water saturation was considered. Water saturation is the most important petrophysical parameter after porosity and permeability because it shows the water fraction in the reservoir rock pores. This will give an estimation about hydrocarbon saturation because pores only can be filled water or hydrocarbon so, if one zone has a very low water saturation value, that zone can be considered as a hydrocarbon zone. The other important petrophysical parameter is net–to–gross ratio. This factor will give an information about net reservoir thickness after applied porosity, shale, and water saturation cutoffs. In this study, the applied porosity cutoff is 15%, the shale volume cutoff is 45%, and the water saturation cutoff is 80%. After applying these cutoffs, the net–to–gross ratio was calculated. The range of net–to–gross ratio is 40%–60%. Finally, all of the 3D models can be used for reservoir decisions. Each parameter represents different feature of the reservoir rocks and combining all of the information will give an accurate estimation for the reservoir.

Figure 6.5 represents facies types of the Kapuni C Sand and Kapuni D Sand formations and shows that the formation contains mostly sandstone, claystone, and limestone that are represented by yellow, turquase, and pink colors respectively. Reservoir zones mostly contain sandstone which is one of the most suitable rock types for production.

Figure 6.7 represents effective porosity of the Kapuni C Sand and Kapuni D Sand formations. Porosity calculated and shale volume considered. Finally, the effective porosity range was obtained. Effective porosity range is more important than total porosity because for reservoir production interconnected pores are considered. In this figure, blue colors represents 20% to 30% range and pink colors represents under 20%. In reservoir zones, effective porosity values higher than the other parts of the formation and this results show that formations have high effective porosity range.

Figure 6.8 represents permeability of the Kapuni C Sand and Kapuni D Sand formations. Red color shows 1000 mD and more, turquase color shows 300 to 500 mD and pink color shows less than 200 mD. Reservoir zones are mostly presented by red colors and these results show the formations are fairly permeable.

Figure 6.9 represents water saturation of the Kapuni C Sand and Kapuni D Sand formations. Red color presents 100% water saturation, green and yellow colors represent 50 to 80% water saturation, blue color represents 20 to 40% water saturation and purple color represents less than 20% water saturation. Reservoir zones mostly represented by purple and blue colors in this model.

Figure 6.10 represents net–to–gross ratio of the Kapuni C Sand and Kapuni D Sand formations. Light colors like green and yellow represent more than 50% and bold colors like blue and purple represent less than 50%. Reservoir zones are mostly represented by light colors.

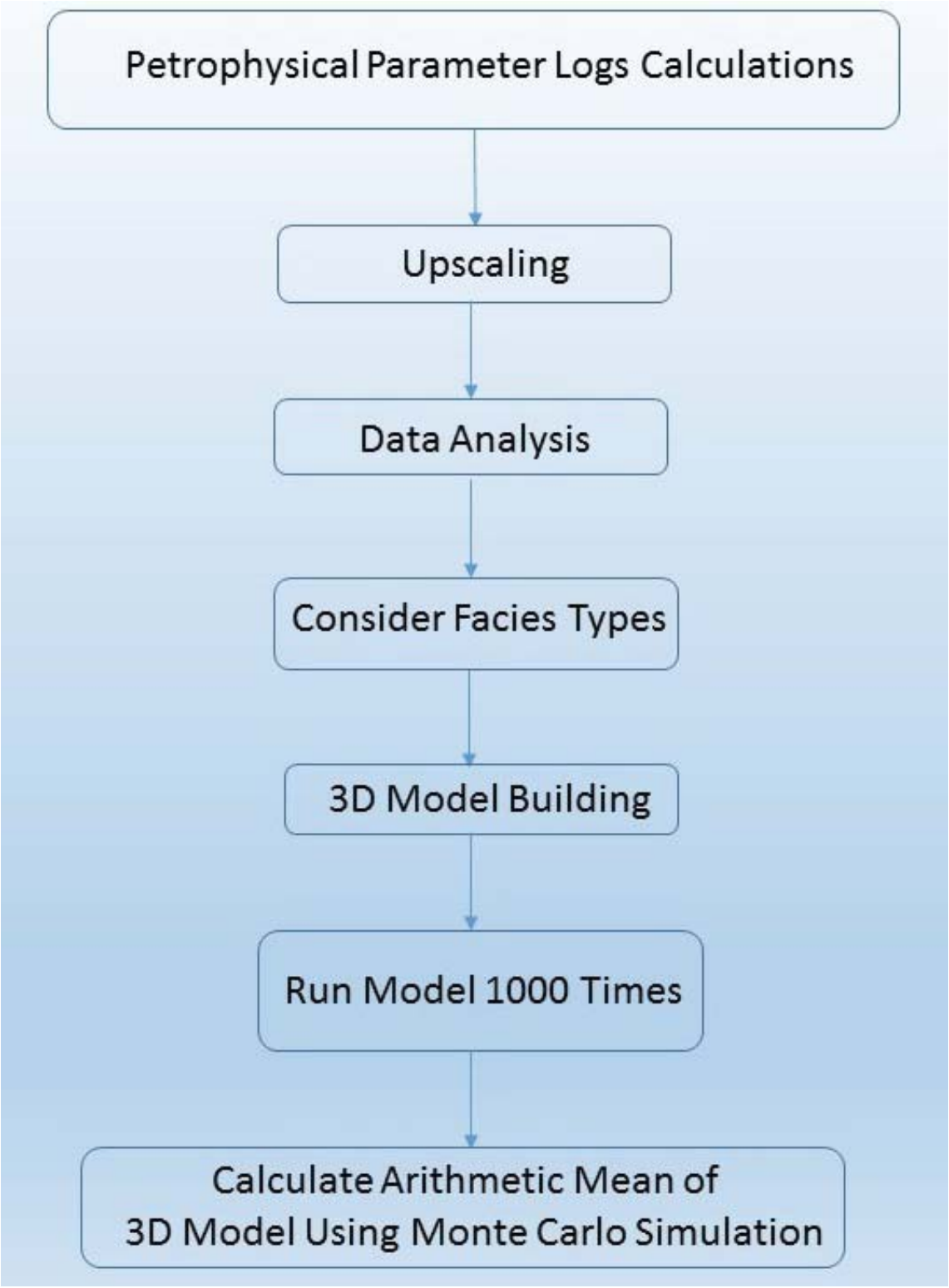

Figure 6.6: 3D Petrophysical Parameters Modeling Workflow

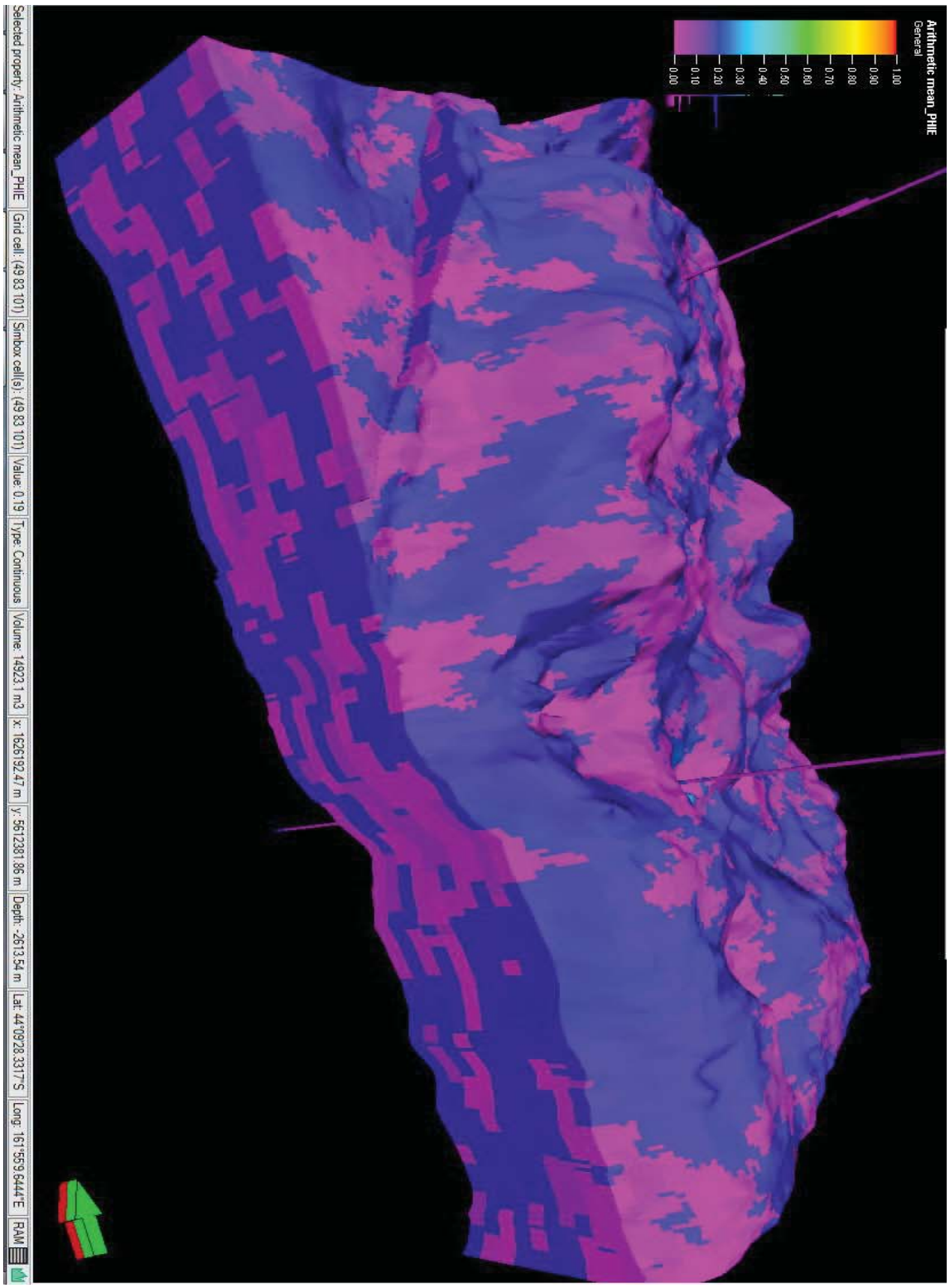

Figure 6.7: 3D Effective Porosity Model

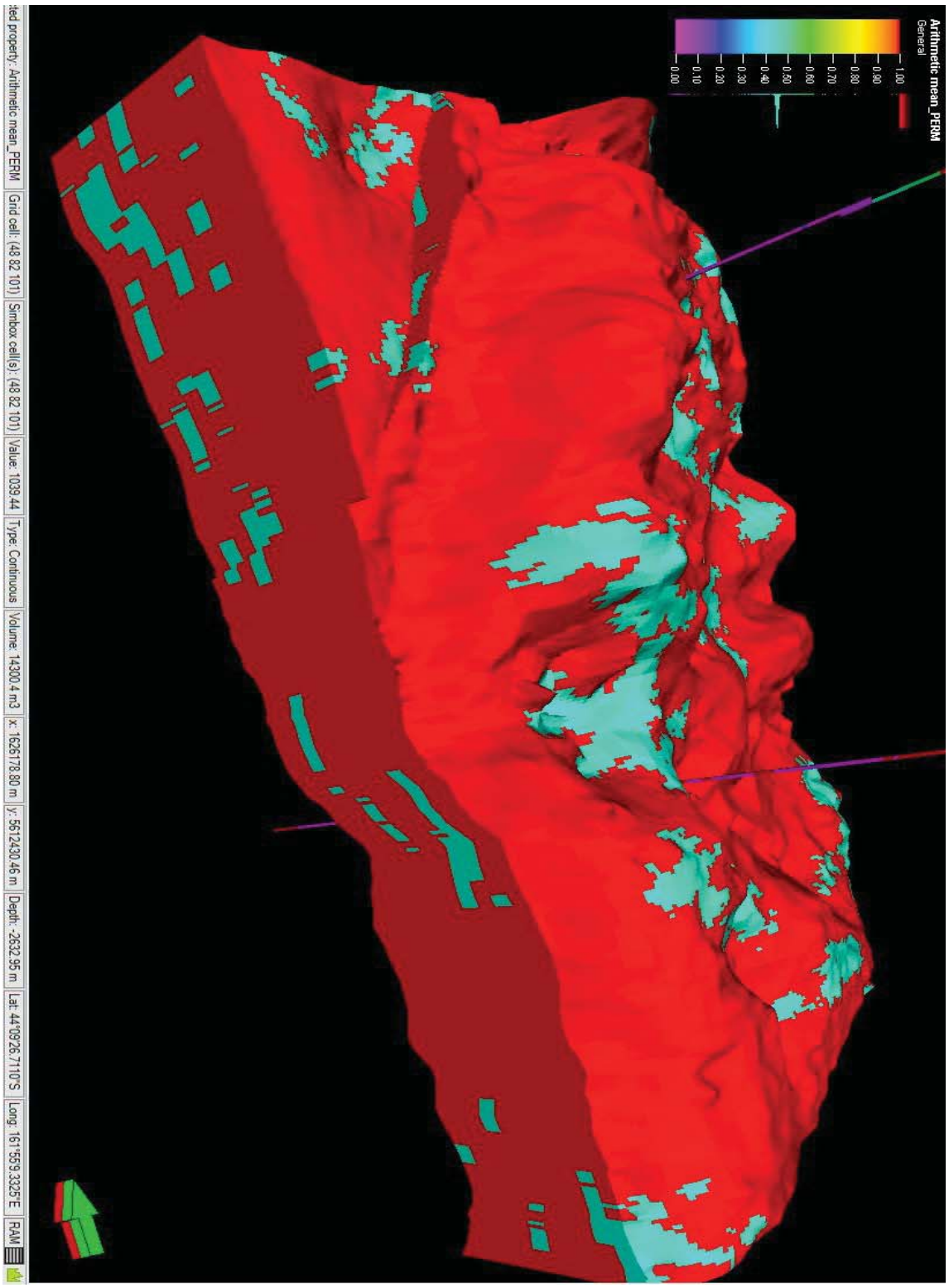

Figure 6.8: 3D Permeability Model

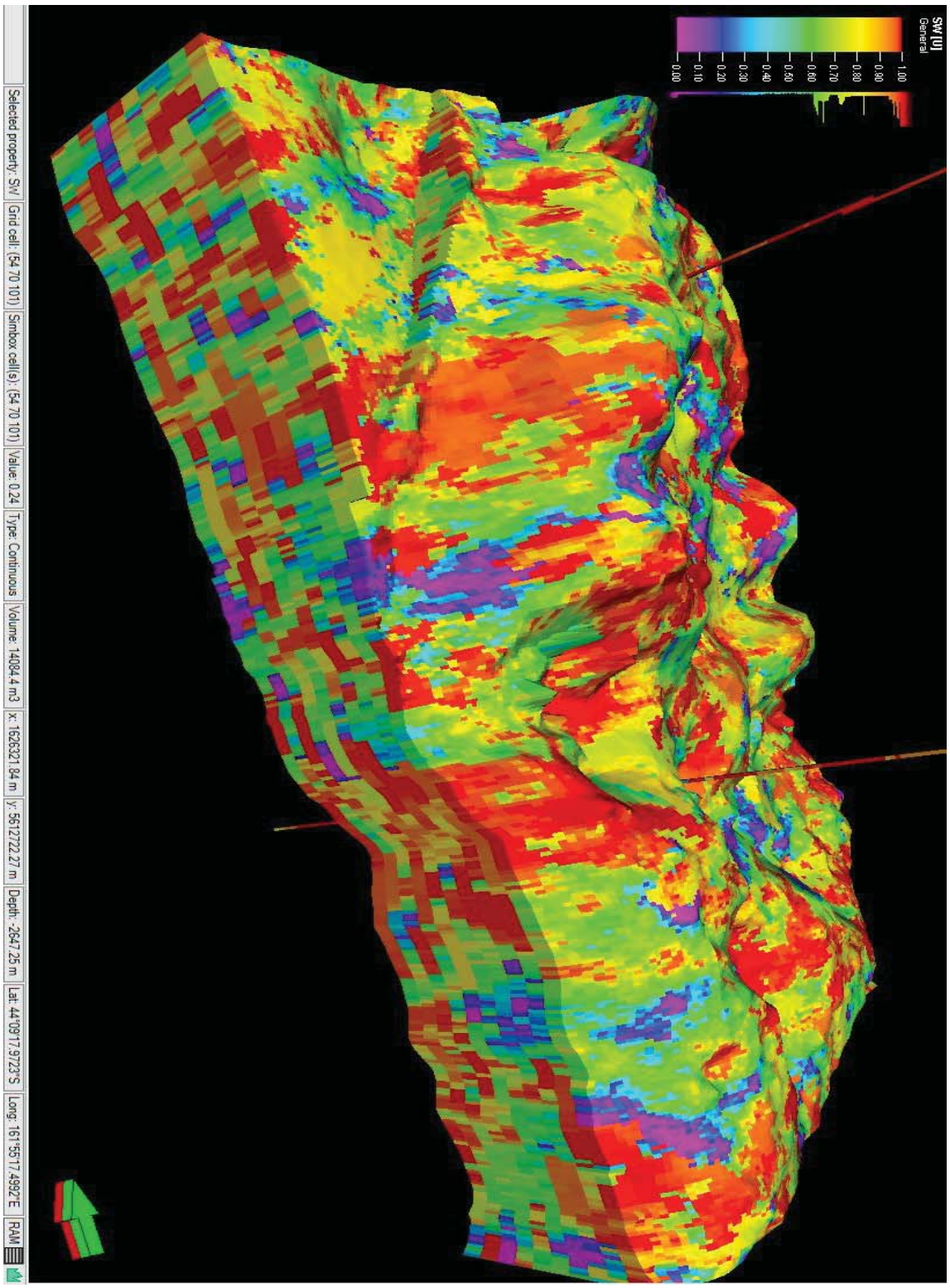

Figure 6.9: 3D Water Saturation Model

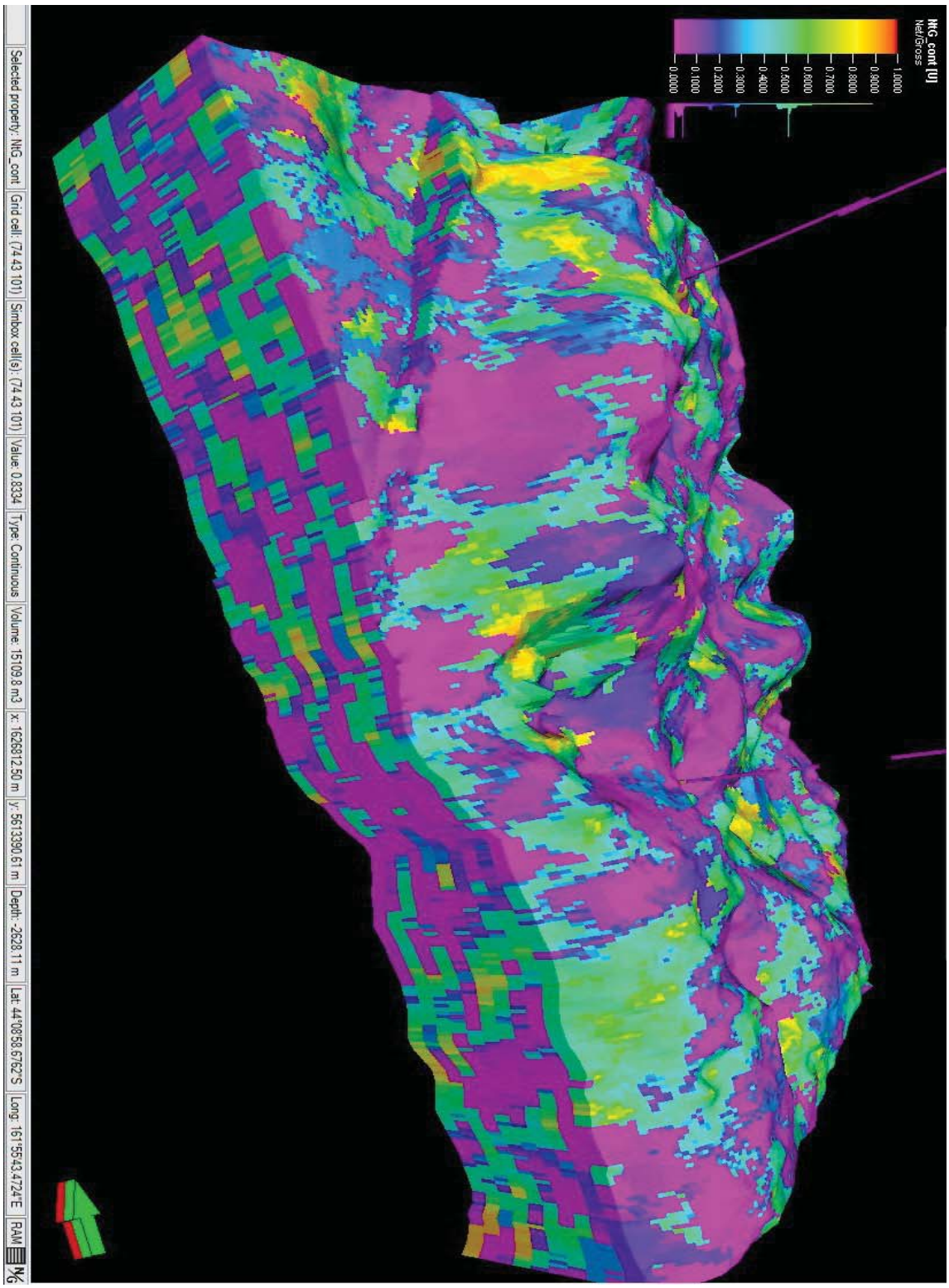

Figure 6.10: 3D Net-to-Gross Ratio Model

7. RESULTS AND DISCUSSION

Well log data and core data were used to find probable oil and gas zones in Maui-B field. The first step was to evaluate both density logs and neutron logs because whenever density logs and neutron logs have a crossover it is a strong sign for gas zones. The next step is a consideration of resistivity logs because hydrocarbons are more resistive than formation water, so if resistivity is high that zone may have hydrocarbons. Then, water saturation needs to be considered because the pores are filled with water or hydrocarbon, so if the water saturation is low, this indicates that there are hydrocarbons in the pores. Also, porosity and permeability must be considered. After porosity is determined, effective porosity must be checked because pores must be interconnected to produce hydrocarbon. The last step is to consider lithology; as facies type is important for the reservoir rock and net–to–gross ratio. Porous and permeable sandstone is the most suitable facies type for a reservoir. In this study, for hydrocarbon zones, all of these analyses were done for five different wells with different locations, and the results were considered. The area contains mostly sandstone, and hydrocarbon zones show a good sign of porosity, permeability, water saturation, and net–to–gross ratio.

For Maui-7 well, all of these analysis were done. Based of these analysis, hydrocarbon zones were determined. Using density log and neutron log crossovers, 87 meters gas zones were detected in both Kapuni C Sand and Kapuni D Sand formations. In addition, using resistivity logs, water saturation log, porosity logs, and permeability log oil zones were detected. The oil zones analysis showed that 17 meters oil zones were detected in total. Both quantitive and qualitative results are given below for the Maui–7 well:

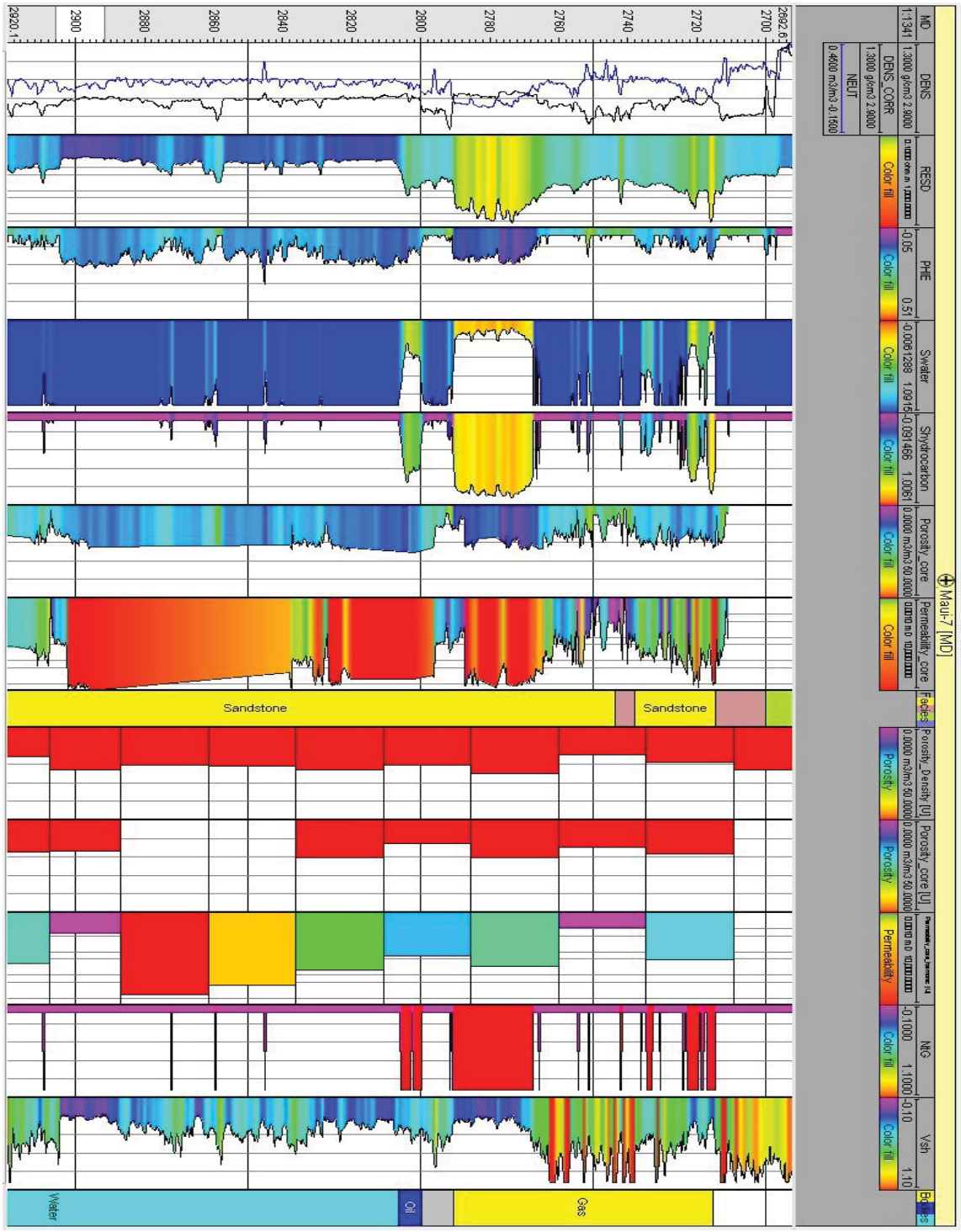

Figure 7.1: Oil and Gas Zones in Kapuni C Sand Formation

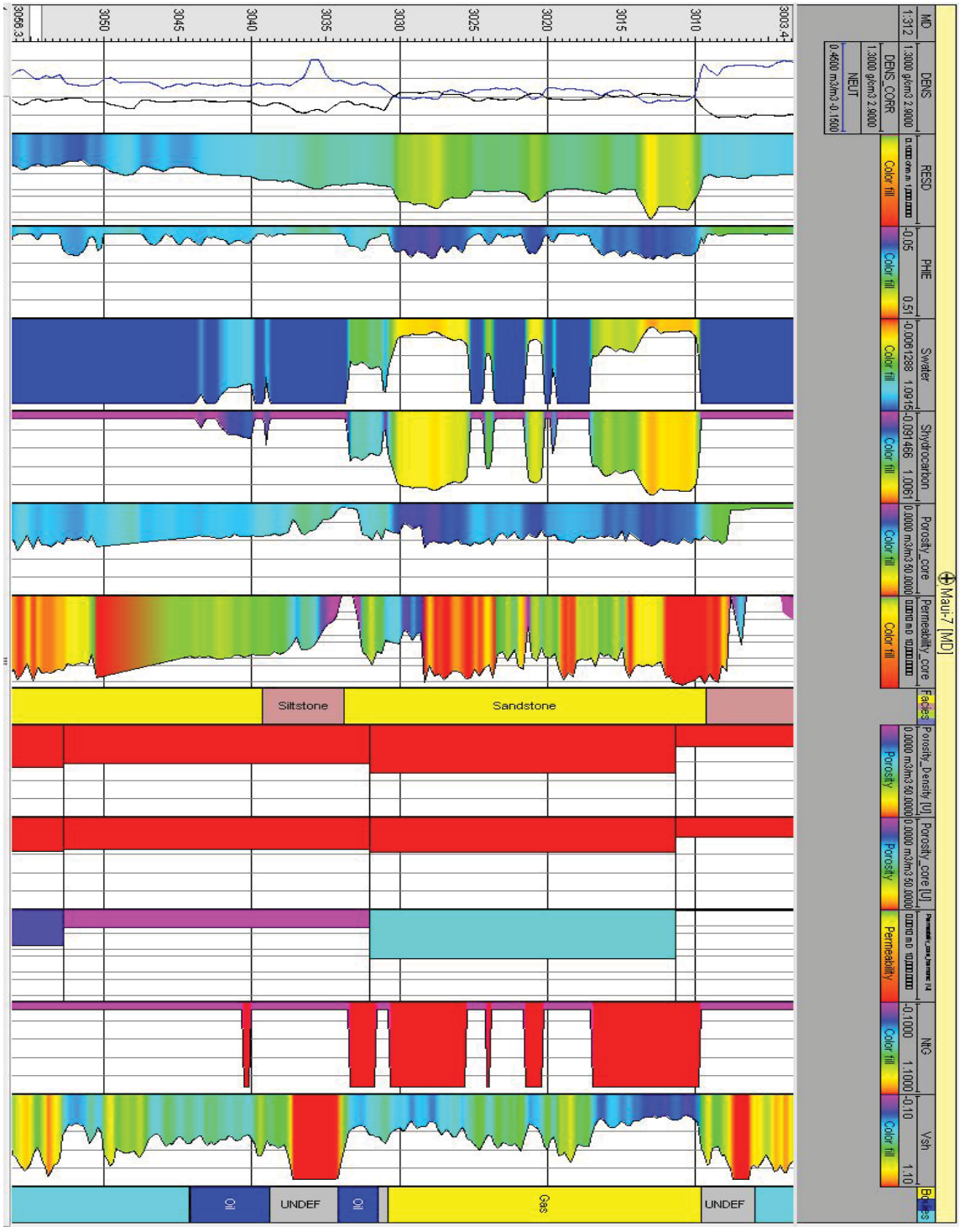

Figure 7.2: Oil and Gas Zones in Kapuni D Sand Formation

Table 7.1: Petrophysical Parameter Calculations from Well Log and Core Data in Maui–7 Well

Name	Minimum	Maximum	Mean
Density Porosity	0	54.8	20.5
Permeability (mD)	0.001	9900	802.1
Water Saturation (%)	8.5	100	96
Volume of Shale (%)	0	100	58

Table 7.2: Petrophysical Parameters Average Values for Oil and Gas Zones in Maui–7 Well

Type	**Depth Range (m)**	**Porosity(%)**	**Permeability (mD)**	**Water Sat. (%)**
Gas	2715–2791	13–33	330–6100	8–33
Oil	2799–2807	20–30	79–3700	9–40
Gas	3009–3030	23–29	96–1400	9–25
Oil	3031–3034	18–30	170–340	33–42
Oil	3038–3044	19–23	330–2200	46–50

Figure 7.1 and Figure 7.2 show both oil and gas zones in Kapuni C Sand and Kapuni D Sand respectively. In addition Table 7.1 shows average petrophysical parameter values from surface to bottom depth of Maui–7 well, also Table 7.2 shows oil and gas zones and these zones' main petrophysical parameter values.

Figure 7.3 compares porosity from core data to porosity calculation from density log. It indicates the porosity values are fairly close to each other in reservoir zones and the picked point which is 2753 meter depth shows that only 2% difference between core data which represents with straight line and log data with represents with circular line.

For oil and gas in place calculations formula 5.11 and 5.12 were used respectively then recovery factor considered for both situation. For these calculations:

Recovery factor (E)= 0.3,

Oil formation volume factor (B_o)= 1.736 rb/stb,

Gas formation volume factor (B_g)= 0.0049 rcf/scf,

Area (A)= 38301.3 acres.

Porosity (ϕ), thickness (h), and water saturation (S_w) were considered for each reservoir zones and sum of the values for both and gas reservoirs are given below.

Original oil in place ($OOIP$)= 136 $mmstb$ and,

Original gas in place ($OGIP$) 1.8 tcf.

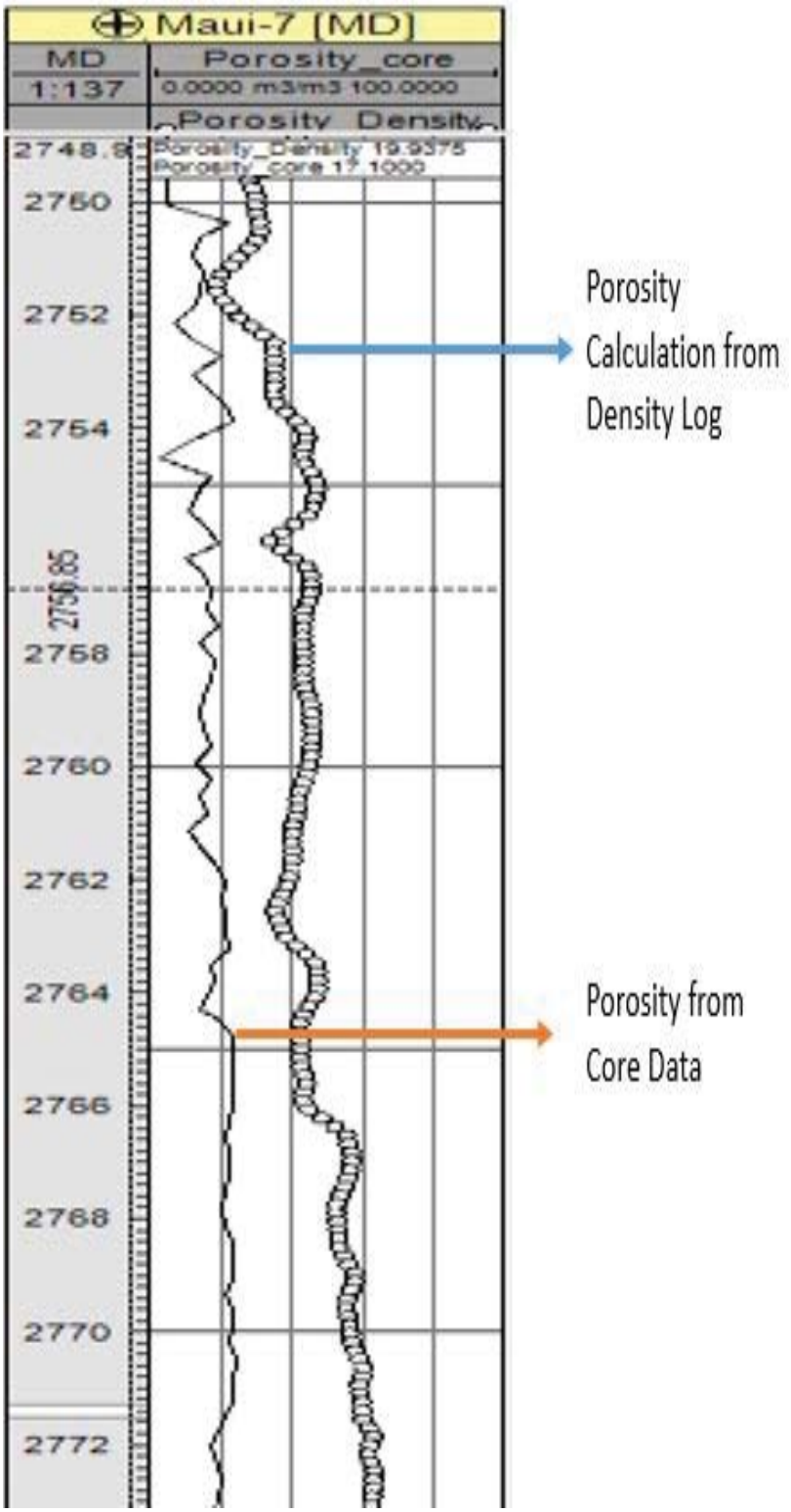

Figure 7.3: Porosity Calculations Comparison between Log Data and Core Data

8. CONCLUSIONS

The aim of this study is to understand and evaluate reservoirs accurately. In this study, three–dimensional seismic data, well log data, and core data were used to analyze reservoir properties and formation properties in the Maui–B field. The three–dimensional seismic data were used to define boundaries of the formation, and well log and core data were calibrated and analyzed to determine oil and gas zones. Based on the petrophysical analysis, reserve estimation was calculated. In addition, the field was bounded by two faults, the Whikiti Fault and Cape Egmont Fault. These large–scale geological structures were modeled using 3D seismic data. Kaimiro–D formation mostly contains sandstone, limestone, and claystone. The total thickness of the gas formations is 97 meters, and the total thickness of oil formations is 19 meters. The hydrocarbon zones were proven by petrophysical analyses that show high porosity, high permeability, low water saturation, low shale volume, and high net–to–gross ratio. As a result, original oil in place ($OOIP$) is 136 $mmstb$ and original gas in place ($OGIP$) is 1.8 tcf. Maui-B field has 30% of the area comparing with the Maui field so comparison between original estimation an estimation which was made in this is very near to each other.

BIBLIOGRAPHY

[1] Taranaki basin yielding large oil and gas discoveries, ResearchGate. [Online]. Available: https://www.researchgate.net/publication/298052766 Taranaki basin yielding large oil and gas discoveries. [Accessed: 18-Jun-2017].

[2] D. Strogen, K. Bland, J. Baur, and P. King, Regional Paleogeography and Implications for Petroleum Prospectively, Taranaki Basin, New Zealand, 2012.

[3] S. Grain, Palaeogeography of a Mid Miocene Turbidite Complex, Moki Formation, Taranaki Basin, New Zealand., 2008.

[4] W. F. H. Pilaar and L. L. Wakefield, Hydrocarbon generation in the Taranaki basin, New Zealand, 1984.

[5] New Zealand: New Zealand Petroleum & Minerals: Ministry of Business. 2014. pp. 2103.

[6] Opportunities for underground geological storage of CO2 in New Zealand - Report CCS -08/8 - Taranaki petroleum fields.

[7] King, P.R., and G.P. Thrasher, Cretaceous-Cenozoic geology and petroleum systems of the Taranaki Basin, New Zealand, Lower Hutt: Institute of Geological & Nuclear Sciences, Institute of Geological & Nuclear Sciences, monograph 13, 1996.

[8] Evolution of faulting and plate boundary deformation in the Southern Taranaki Basin, New Zealand.

[9] King, P.R., and G.P. Thrasher, Cretaceous-Cenozoic geology and petroleum systems of the Taranaki Basin, New Zealand, Lower Hutt: Institute of Geological & Nuclear Sciences, Institute of Geological & Nuclear Sciences, monograph 13, p.243, 1996.

[10] Higgs, K.E., P.R. King, J.I. Raine, R. Sykes, G.H. Browne, E.M Crouch, and J.R. Baur, Sequence stratigraphy and controls on reservoir sandstone distribution in an Eocene marginal marine-coastal plain fairway, Taranaki Basin, New Zealand, Marine and Petroleum Geology, 32(1): p.110-137, 2012.

[11] Structural Modeling of the Maui Gas Field, Taranaki Basin, New Zealand.

[12] Z. Bassiouni, Theory, Measurement, and Interpretation of Well Logs. Henry L. Doherty Memorial Fund of AIME, Society of Petroleum Engineers, 1994.

[13] G. Nie, H. Xu, and others, Static SP measurement tool and its field applications, in SPWLA 50th Annual Logging Symposium, 2009.

[14] H. G. Doll and others, The SP log: Theoretical analysis and principles of interpretation, Transactions of the AIME, vol. 179, no. 01, pp. 146185, 1949.

[15] D. W. Hilchie and others, Caliper logging-theory and practice, The Log Analyst, vol. 9, no. 01, 1968.

[16] N. Dowla, J. C. Rasmus, S. Srivastava, D. Ellis, C. Fulton, and others, Caliper and borehole geometry determinations from logging while drilling measurements and images, in SPWLA 47th Annual Logging Symposium, 2006.

[17] G. Asquith and D. Krygowski, Basic well log analysis, 2nd edn, AAPG methods in exploration series, American Association of Petroleum Geologists, Tulsa, OK, 2004.

[18] D. V. Ellis, C. R. Case, J. M. Chiaramonte, and others, Tutorial-porosity from neutron logs I-Measurement, Petrophysics, vol. 44, no. 06, 2003.

[19] G. J. Lasinio, Michael J. Pyrcz, Clayton V. Deutsch: Geostatistical reservoir modeling, METRON, vol. 73, no. 1, pp. 149150, 2015.

[20] C. S. Bristow and B. J. Williamson, Spectral gamma ray logs: core to log calibration, facies analysis and correlation problems in the Southern North Sea, Geological Society, London, Special Publications, vol. 136, no. 1, pp. 17, Jan. 1998.

[21] G. B. Asquith, D. Krygowski, and C. R. Gibson, Basic well log analysis, vol. 16. American association of petroleum geologists Tulsa, 2004.

[22] Permeability - AAPG Wiki. [Online]. Available: http://wiki.aapg.org/Permeability. [Accessed: 17-Jun-2017].

[23] B. Rafik and B. Kamel, Prediction of permeability and porosity from well log data using the nonparametric regression with multivariate analysis and neural network, Hassi RMel Field, Algeria, Egyptian Journal of Petroleum, 2016.

[24] H. Darcy, Les fontaines publique de la ville de Dijon, Dalmont, Paris, vol. 647, 1856.

[25] Crains Petrophysical Handbook - Water Saturation Basics. [Online]. Available: https://www.spec2000.net/14-swbasics.htm. [Accessed: 17-Jun-2017].

[26] Poupon, A., & Gaymard, R. (1970, January 1). The Evaluation Of Clay Content From Logs. Society of Petrophysicists and Well-Log Analysts.

[27] M. H. Kamel and W. M. Mabrouk, Estimation of shale volume using a combination of the three porosity logs, Journal of Petroleum Science and Engineering, vol. 40, no. 3, pp. 145157, Dec. 2003.

[28] R. H. Snyder and others, A Review of the Concepts and Methodology of Determining Net Pay, in Fall Meeting of the Society of Petroleum Engineers of AIME, 1971.

[29] P. F. Worthington and others, Net PayWhat Is It? What Does It Do? How Do We Quantify It? How Do We Use It?, SPE Reservoir Evaluation & Engineering, vol. 13, no. 05, pp. 812822, 2010.

[30] Upscaling of grid properties in reservoir simulation -. [Online]. Available: http://petrowiki.org/Upscaling of grid properties in reservoir simulation. [Accessed: 17-Jun-2017].

[31] Schlumberger. Petrel Property Modeling, 16th Edition. Schlumberger. VitalBook file.

[32] A. Kumar, C. L. Farmer, G. R. Jerauld, D. Li, and others, Efficient upscaling from cores to simulation models, in SPE Annual Technical Conference and Exhibition, 1997.

[33] J. M. Yarus, R. L. Chambers, and others, Practical geostatistics-an armchair overview for petroleum reservoir engineers, Journal of Petroleum Technology, vol. 58, no. 11, pp. 7886, 2006.

[34] V. N. Simlote, S. A. Nikolayenko, and others, Dealing with uncertainty: Geostatistics and the new era in reservoir studies, in SPE India Oil and Gas Conference and Exhibition, 1998.

[35] E. Gringarten and C. V. Deutsch, Teachers aide variogram interpretation and modeling, Mathematical Geology, vol. 33, no. 4, pp. 507534, 2001.

VITA

Aziz Mennan was born in Osmaniye, Turkey. He received his Bachelor of Science degree in 2012 in the Department of Geological Engineering, Cukurova University, Adana, Turkey. He completed an internship in The Turkish Petroleum Corporation in Adiyaman, Turkey, in 2011. He started his Master of Science in Geological Engineering in 2012 from the same university. He started to work in a road construction in 2013 from TEMAT company, in Kastamonu, Turkey. He was awarded a scholarship from Turkish Petroleum Corporation to pursue his Master of Science in reservoir modeling in the USA in 2014. He studied in Ohio Program of Intensive English at Ohio University from August 2014 to July 2015. He started his Master of Science in the Petroleum Engineering department at Missouri University of Science and Technology in August 2015 in Rolla, Missouri, USA. During his graduate studies, he worked on well log interpretation and three–dimensional reservoir property modeling of Maui-B Field, Taranaki Basin, New Zealand. While he was doing his graduate studies, he had a poster presentation about his thesis topic at Cukurova University Department of geological Engineering 40th Year Geology Symposium in 2017 and Society of Petroleum Engineers Energy Symposium at Missouri University of Science and Technology in 2017. He presented his research at the 4^{th} annual Caspian Technical Conference and Exhibition in Baku, Azerbaijan in November 2017. He received his Master of Science in Department of Petroleum Engineering in December 2017.